

1  
2  
3  
4  
5  
6  
7  
8  
9  
10  
11  
12  
13  
14  
15  
16  
17  
18  
19  
20

**Overcoming barriers to enable convergence research by integrating ecological and climate sciences: The NCAR-NEON system Version 1**

Danica L. Lombardozzi<sup>1§\*</sup>, William R. Wieder<sup>1,2,§,\*</sup>, Negin Sobhani<sup>1</sup>, Gordon B. Bonan<sup>1</sup>, David Durden<sup>3</sup>, Dawn Lenz<sup>3</sup>, Michael SanClements<sup>3</sup>, Samantha Weintraub-Leff<sup>3</sup>, Edward Ayres<sup>3</sup>, Christopher R. Florian<sup>3</sup>, Kyla Dahlin<sup>4</sup>, Sanjiv Kumar<sup>5</sup>, Abigail L. S. Swann<sup>6</sup>, Claire Zarakas<sup>6</sup>, Charles Vardeman<sup>7</sup>, Valerio Pascucci<sup>8</sup>

<sup>1</sup> Climate and Global Dynamics Laboratory, National Center for Atmospheric Research, Boulder CO, USA.

<sup>2</sup> Institute of Arctic and Alpine Research, University of Colorado Boulder, Boulder CO, USA.

<sup>3</sup> National Ecological Observatory Network, Battelle. Boulder CO, USA.

<sup>4</sup> Michigan State University, East Lansing MI, USA.

<sup>5</sup> College of Forestry, Wildlife and Environment, Auburn University, Auburn AL, USA.

<sup>6</sup> University of Washington, Seattle WA, USA.

<sup>7</sup> Center for Research Computing, University of Notre Dame, Notre Dame, IN, USA

<sup>8</sup> Scientific Computing and Imaging Institute, University of Utah, Salt Lake City, UT, USA

<sup>§</sup> Contributed equally as lead authors.

\* Correspondence to: [dll@ucar.edu](mailto:dll@ucar.edu) and [wwieder@ucar.edu](mailto:wwieder@ucar.edu)

## 21 **Abstract**

22           Global change research demands a convergence among academic disciplines to understand  
23 complex changes in Earth system function. Limitations related to data usability and computing  
24 infrastructure, however, present barriers to effective use of the research tools needed for this cross-  
25 disciplinary collaboration. To address these barriers, we created a computational platform that pairs  
26 meteorological data and site-level ecosystem characterizations from the National Ecological Observatory  
27 Network (NEON) with the Community Terrestrial System Model (CTSM) that is developed with university  
28 partners at the National Center for Atmospheric Research (NCAR). This NCAR-NEON system features a  
29 simplified user interface that facilitates access to and use of NEON observations and NCAR models. We  
30 present preliminary results that compare observed NEON fluxes with CTSM simulations and describe  
31 how the collaboration between NCAR and NEON that can be used by the global change research  
32 community improves both the data and model. Beyond datasets and computing, the NCAR-NEON  
33 system includes tutorials and visualization tools that facilitate interaction with observational and model  
34 datasets and further enable opportunities for teaching and research. By expanding access to data,  
35 models, and computing, cyberinfrastructure tools like the NCAR-NEON system will accelerate integration  
36 across ecology and climate science disciplines to advance understanding in Earth system science and  
37 global change.

## 38 **Short Summary**

39 We present a novel cyberinfrastructure system that uses National Ecological Observatory Network  
40 measurements to run Community Terrestrial System Model point simulations in a containerized system.  
41 The simple interface and tutorials expand access to data and models used in Earth system research by  
42 removing technical barriers and facilitating research, educational opportunities, and community  
43 engagement. The NCAR-NEON system enables convergence of climate and ecological sciences.

## 44 **1. Introduction**

45           Earth system science aims to deepen understanding of interactions between natural and social  
46 systems and their responses to global change. As such, the collective understanding of changes in Earth  
47 system function in response to global change drivers requires a convergence among scientific disciplines,  
48 including physical and natural sciences (Kyker-Snowman et al. 2022). This research combines a variety  
49 of complex observational data with ever more sophisticated computational models. Notably, Earth System  
50 Models (ESMs) are essential tools for assessing and predicting our changing environment (Bonan and  
51 Doney 2018), but limitations related to data usability and access to computing infrastructure present  
52 barriers to effective use of these research tools (Fer et al. 2021). Addressing these barriers is critical to  
53 engage the broad, cross-disciplinary communities that are required for Earth system science research,

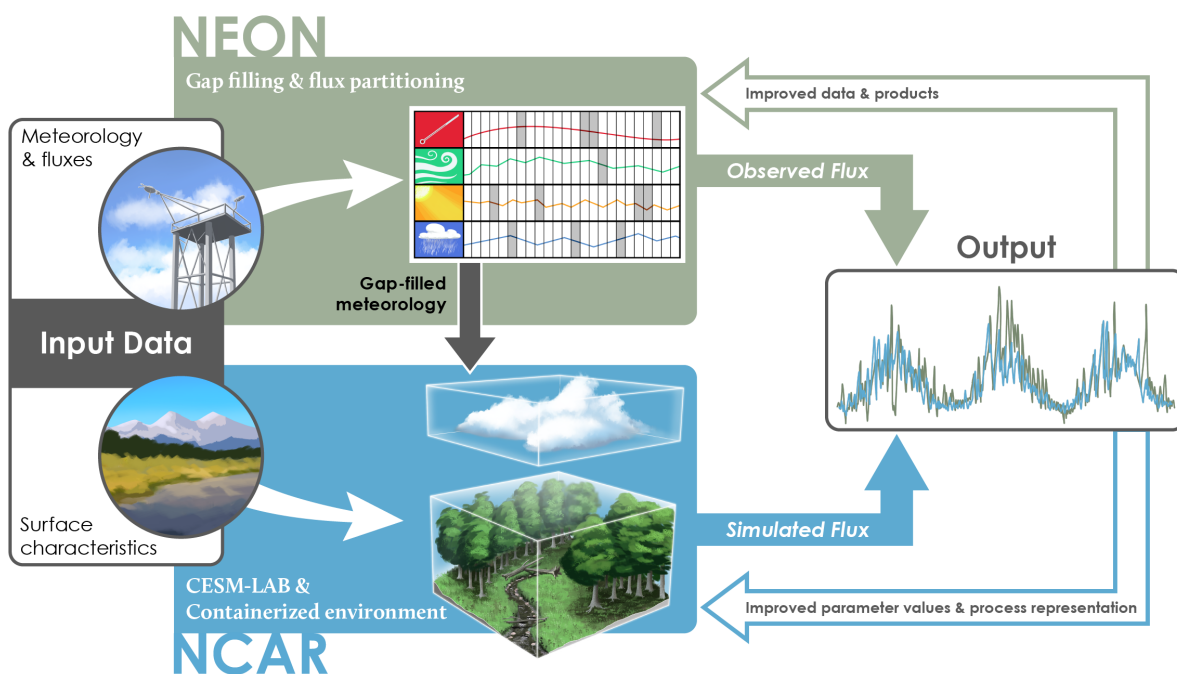
54 education, and training (NASEM, 2022). We feel that tractable progress can be made to reduce these  
55 data and technical barriers to better understand and project changes in Earth system function under  
56 global change.

57         The availability, discoverability, and usability of observational data are essential to running,  
58 calibrating, and validating models. For example, the scientific advancements made in measuring eddy  
59 covariance (EC) fluxes have been critical to the development, evaluation, and improvement of the  
60 representation of terrestrial ecosystems in ESMs. Initially, model-data comparisons were limited to short,  
61 intensive field campaigns extending over a few weeks (Bonan et al. 1997), but this grew to comparison  
62 with flux network datasets extending over several years at multiple sites (Stöckli et al. 2008), and  
63 comparison with globally gridded flux products (Bonan et al. 2011; Jung et al. 2020). Flux tower data sets  
64 continue to provide essential information for land model development and evaluation (Best et al. 2015;  
65 Lawrence et al. 2019). Notably, single-point simulations can use EC measurements to facilitate more  
66 rapid model development and testing of ecological hypotheses (Bonan et al. 2012; Burns et al 2018;  
67 Collier et al. 2018; Swenson et al. 2019; Wieder et al. 2017). An explosion of EC measurements and  
68 strong network coordination make these data easier to find (Beringer et al. 2022, Durden et al. 2020;  
69 Pastorello et al. 2020, Novick et al. 2018), but the need to perform additional data processing prior to use  
70 presents barriers to integrating ecological observations into land model development and evaluation.  
71 These barriers include gap filling associated meteorological data, assessing EC flux data quality, and  
72 persistent challenges in discovering and harmonizing complementary data – including information about  
73 vegetation and soils at EC tower sites. Our work seeks to provide a framework to address these data  
74 challenges to facilitate the integration of local meteorology, EC flux measurements, and ecosystem  
75 characterizations in the development and evaluation of land models that are used for Earth system  
76 prediction and global change research.

77         Beyond these data challenges, barriers to accessing and using computing infrastructure also  
78 impede broader community engagement with tools that are central to global change research. This limits  
79 the participation of scientists from environmental science, ecology, and agroecology, which are  
80 fundamental components of the Earth system, in the development and use of ESMs. The Community  
81 Earth System Model (CESM; Hurrell et al. 2013; Danabasoglu et al. 2020) has a long history of being  
82 freely and openly available to users, yet several barriers related to training, cyberinfrastructure, and data  
83 integration have hampered broader adoption and use of this model by a wide range of researchers. Thus,  
84 model code may be publicly available, but access to computing resources and the associated technical  
85 expertise needed to use them presents barriers to engaging a diverse, cross-disciplinary community of  
86 model users who can harness these powerful tools for research and teaching. We contend that broader  
87 engagement across scientific disciplines is critical to improving the representation of Earth system  
88 processes and their likely responses to global change.

89         This work overcomes some of the barriers to the use of ESMs in ecology by creating an  
90 integrated 'NCAR-NEON system'. This system combines meteorological data and site-level ecosystem

91 characterizations from the National Ecological Observatory Network (NEON) with the Community  
 92 Terrestrial System Model (CTSM), an extension of the Community Land Model (CLM5; Lawrence et al.  
 93 2019). CTSM is the terrestrial component of CESM, which is developed with university partners at the  
 94 National Center for Atmospheric Research (NCAR; Fig. 1). The NCAR-NEON system also features a  
 95 simplified user interface that facilitates access to and use of NEON observations and NCAR models. By  
 96 developing this NCAR-NEON system, we aim to enable the convergence of climate and ecological  
 97 sciences by providing accessible cyberinfrastructure, quality-controlled datasets from NEON, and tutorials  
 98 for analyzing and visualizing observed and simulated data. We describe development of the NCAR-  
 99 NEON system, present results comparing observed NEON fluxes with simulations from CTSM, and  
 100 outline opportunities that the system enables for research and education across research networks and  
 101 scientific disciplines.



102  
 103 **Figure 1.** A conceptual diagram illustrating the integration of NEON data and NCAR modeling enabled through the  
 104 NCAR-NEON system. NEON meteorological measurements are gap-filled using redundant streams and used as inputs  
 105 for single point simulations with the Community Terrestrial Systems Model (CTSM). Additional NEON observations are  
 106 used as input data to the model, including surface characteristics of vegetation (e.g., mapping to simulated plant  
 107 functional types, PFTs) and the soil properties (soil texture, organic matter content, and depth to bedrock, if < 2m).  
 108 Simulations with CTSM are conducted in CESM-Lab, a computing environment that runs in a container or with cloud  
 109 computing resources, which includes model code and analysis tools. Simulated data is compared with observed fluxes  
 110 using visualization scripts that are provided within CESM-Lab to improve both observed data products, model  
 111 parameterization, and model processes representation.

112

113 **2. Methods**

114 **2.1 NEON Data**

115 NEON is a research network comprising 81 monitoring sites (47 terrestrial, 34 aquatic) that are  
 116 collecting standardized, open data across the major ecosystems of the United States (Table S1). NEON's  
 117 data products are highly complementary to land models, providing high quality and standardized data for  
 118 soil, vegetation, and atmosphere states and fluxes across vast spatiotemporal scales with high  
 119 throughput instrumented systems data and spatially expansive remote sensing data (Hinckley et al. 2016;  
 120 Balch et al. 2020; Durden et al. 2020). Each of the 47 NEON terrestrial sites includes an EC tower to  
 121 determine the surface-atmosphere exchange of momentum, heat, water, and CO<sub>2</sub>, alongside meteorology  
 122 (precipitation, wind speed, humidity, temperature), atmospheric composition (water vapor and CO<sub>2</sub>  
 123 concentrations and isotopic ratios), and soil sensor assemblies measuring depth-resolved soil  
 124 temperature and moisture at several locations in the EC tower footprint (Metzger et al. 2019). In this  
 125 preliminary effort to bring NEON measurements and NCAR modeling together we use NEON data for: 1)  
 126 Meteorological inputs that are gap filled and provide local atmospheric boundary condition inputs to  
 127 CTSM; 2) Vegetation and soil properties; and 3) Eddy covariance fluxes to compare observed and  
 128 simulated results (Fig. 1, Table 1), with prototype data available through the NEON data portal (NEON  
 129 2023).

131 **Table 1.** NEON data product name, data product use in CTSM, NEON data product ID, and Digital Object  
 132 Identifier (DOI). Data products were used for meteorological inputs and surface characterization, which are  
 133 inputs needed to run CTSM, and for model evaluation.

Data Product Name	Data Product Use	Data Product ID	DOI
Precipitation	Meteorological input	DP1.00006.001	<a href="https://doi.org/10.48443/6wkc-1p05">https://doi.org/10.48443/6wkc-1p05</a>
Relative humidity	Meteorological input	DP1.00098.001	<a href="https://doi.org/10.48443/w9nf-k476">https://doi.org/10.48443/w9nf-k476</a>
Shortwave and longwave radiation (net radiometer)	Meteorological input	DP1.00023.001 *DP1.00024.001 *DP1.00014.001	<a href="https://doi.org/10.48443/stbf-bh38">https://doi.org/10.48443/stbf-bh38</a> <a href="https://doi.org/10.48443/8a01-0677">https://doi.org/10.48443/8a01-0677</a> <a href="https://doi.org/10.48443/hv8e-5696">https://doi.org/10.48443/hv8e-5696</a>
Barometric pressure	Meteorological input	DP1.00004.001 *DP4.00200.001	<a href="https://doi.org/10.48443/zr37-0238">https://doi.org/10.48443/zr37-0238</a> <a href="https://doi.org/10.48443/7cqp-3j73">https://doi.org/10.48443/7cqp-3j73</a>
Wind speed	Meteorological input	DP4.00200.001 *DP1.00001.001	<a href="https://doi.org/10.48443/7cqp-3j73">https://doi.org/10.48443/7cqp-3j73</a> <a href="https://doi.org/10.48443/77n6-eh42">https://doi.org/10.48443/77n6-eh42</a>
Air temperature	Meteorological input	DP4.00200.001 *DP1.00003.001	<a href="https://doi.org/10.48443/7cqp-3j73">https://doi.org/10.48443/7cqp-3j73</a> <a href="https://doi.org/10.48443/q16j-sn13">https://doi.org/10.48443/q16j-sn13</a>
Forcing height	Meteorological input	DP4.00200.001	<a href="https://doi.org/10.48443/7cqp-3j73">https://doi.org/10.48443/7cqp-3j73</a>
Soil physical and chemical properties, Megapit	Soil property characterization	DP1.00096.001	<a href="https://doi.org/10.48443/10dn-8031">https://doi.org/10.48443/10dn-8031</a>
Dominant vegetation type	Surface characterization	Manually Assigned	
Bundled data pro	Model Evaluation	DP4.00200.001	<a href="https://doi.org/10.48443/7cqp-3j73">https://doi.org/10.48443/7cqp-3j73</a>

ducts - eddy covariance		*DP1.00023.001	
Net radiation	Model Evaluation	DP1.00023.001 *DP1.00014.001	<a href="https://doi.org/10.48443/stbf-bh38">https://doi.org/10.48443/stbf-bh38</a> <a href="https://doi.org/10.48443/hv8e-5696">https://doi.org/10.48443/hv8e-5696</a>
Photosynthetically Active Radiation (PAR)	Model Evaluation	DP1.00024.001 *DP1.00023.001 *DP1.00014.001	<a href="https://doi.org/10.48443/8a01-0677">https://doi.org/10.48443/8a01-0677</a> <a href="https://doi.org/10.48443/stbf-bh38">https://doi.org/10.48443/stbf-bh38</a> <a href="https://doi.org/10.48443/hv8e-5696">https://doi.org/10.48443/hv8e-5696</a>
Direct and Diffuse Radiation	Model Evaluation	DP1.00014.001	<a href="https://doi.org/10.48443/hv8e-5696">https://doi.org/10.48443/hv8e-5696</a>
Soil water content and water salinity	Model Evaluation	DP1.00094.001	<a href="https://doi.org/10.48443/ghry-qw46">https://doi.org/10.48443/ghry-qw46</a>

134 \*Indicates the data product was used in the redundant stream gap-filling to fill primary data product

135 2.1.1 Meteorological inputs

136 Generating the gap-filled meteorological data that are required for single-point simulations with  
137 land models can be time consuming and requires expertise in micro-meteorology that land model users  
138 and developers may not have. Thus, the modeling community historically relied on external efforts like  
139 FLUXNET synthesis databases to provide gap-fill meteorological measurements at eddy-flux sites (e.g.,  
140 La Thuile or FLUXNET2015; Pastorello et al 2020). Downloading and processing these datasets into a  
141 format that is usable by the model is also time consuming, and often the flux measurements are not  
142 paired with information about local vegetation or soil properties that are easy to discover or digest.  
143 Collectively, these factors create barriers for use and latencies in updating the EC observational data that  
144 are used in single point simulations. The NCAR-NEON system aims to remove some of these barriers.

145 NEON meteorological input data used to run CTSM are summarized in Table 1, and gap-filled  
146 using publicly available code (Table 2). While NEON is highly standardized, a few differences in  
147 instrumentation exist between NEON Core (representative of the predominant natural ecosystem of each  
148 respective Domain) and gradient sites (representing other endmember conditions in each respective  
149 Domain). For example, core NEON sites measure precipitation with Double-fenced Intercomparison  
150 Reference gauges, while gradient sites all have tipping buckets (Metzger et al. 2019). Accounting for  
151 these site-specific sensor configurations and variation in their associated data streams is the first step in  
152 providing usable meteorological inputs to CTSM. The meteorological inputs to CTSM must be continuous,  
153 therefore, additional gap filling of missing data is required. Additionally, the EC system collects data  
154 necessary to calculate fluxes of energy, water vapor, and CO<sub>2</sub>. The NEON site design builds in some  
155 redundancy in observations with profiles of incoming radiation, wind, temperature, water vapor, and CO<sub>2</sub>  
156 concentrations measured at different heights on each NEON tower (Metzger et al. 2019). These data  
157 redundancies allow for a robust initial gap-filling using linear regressions among the primary and  
158 redundant data streams to correct for instrument or location differences. For example, if wind speed or air  
159 pressure measurements from the tower top are missing, we gap-fill with the value from the redundant  
160 data stream (typically measured at a lower tower height) corrected by the linear relationship with the

161 primary sensor data. If multiple redundant data streams are available, the best fit regression with data  
 162 available is used to determine the gap-filled value for each missing data point.

163 After gap-filling using related data stream regression, some range thresholds and proper unit  
 164 conversions are applied to prepare the meteorological data for processing through the ReddyProc R  
 165 package following the gap-filling workflow outlined in Wutzler et al. (2018). After using related data stream  
 166 regressions, the meteorological data are checked for additional gaps, and gap-filling is performed using  
 167 one of three additional gap-filling methodologies that include look-up table (Falge et al. 2001), mean  
 168 diurnal course, and marginal distribution sampling (Moffat et al. 2007; Reichstein et al. 2005). The gap-  
 169 filling method is tracked and provided as a flag with the data to allow users to assess data with various  
 170 methodology restrictions. The meteorological data streams are then converted to units required by CTSM  
 171 and output to cloud storage in Network Common Data Form (netCDF) format with associated metadata to  
 172 fully describe data provenance and formatting. At most sites data coverage spans January 1, 2018,  
 173 through December 31, 2021, but as more NEON data are collected these files will also be updated in  
 174 near-real time, thus removing barriers associated with processing flux tower data and reducing latencies  
 175 in using new data as they are collected. Tables S1 and S2 provides a list of all the sites where input data  
 176 have been successfully gap-filled and notes any potential data quality issues.

177

178

**Table 2.** List of helpful websites created for the NCAR-NEON system, their contents and a url address for each.

Name	Contents
Project Home Page	Main landing page for users interested in learning more about the project  URL: <a href="https://neoncollab.ucar.edu">https://neoncollab.ucar.edu</a>
Tutorial	Tutorial that introduces running CTSM at NEON tower sites in the CESM-Lab container  URL: <a href="https://ncar.github.io/ncar-neon-books/notebooks/NEON_Simulation_Tutorial.html">https://ncar.github.io/ncar-neon-books/notebooks/NEON_Simulation_Tutorial.html</a>
Interactive Visualizations	Interactive plots that allow users to explore data produced by the NCAR-NEON system without running the model or downloading data  URL: <a href="https://ncar.nationalsciencedatafabric.org/neon-demo/v1/">https://ncar.nationalsciencedatafabric.org/neon-demo/v1/</a>
Processing NEON data	Docker image with scripts used for gap filling meteorological data, flux partitioning, and formatting NEON datasets

<a href="https://quay.io/repository/ddurden/ncar-neon">URL: https://quay.io/repository/ddurden/ncar-neon</a>	
DiscussCESM Forum	Discussion forum bulletin boards for questions related to CESM including CESM-Lab and CTSM
<a href="https://bb.cgd.ucar.edu/cesm/">URL: https://bb.cgd.ucar.edu/cesm/</a>	
CTSM Repository	Code base, technical documentation and information related to CTSM
<a href="https://github.com/ESCOMP/CTSM">URL: https://github.com/ESCOMP/CTSM</a>	
NEON Prototype Data	NEON prototype datasets, which include the gap filled meteorological data for flux partitioned data used for model input and evaluations
<a href="https://data.neonscience.org/prototype-datasets/0a56e076-401e-2e0b-97d2-f986e9264a30">URL: https://data.neonscience.org/prototype-datasets/0a56e076-401e-2e0b-97d2-f986e9264a30</a>	

179

180



181 *2.1.2. Soil and vegetation properties*

182 Basic information on edaphic properties is needed in the pedotransfer functions that describe soil  
183 thermal and hydraulic properties in CTSM. Although NEON has several soil sampling datasets, we used  
184 information from the Megapit characterization of soil physical and chemical properties in CTSM because it  
185 contains more information about deep soil horizons (> 1 m depth; Table 1) from a single soil pit at each  
186 site. Megapit samples were collected by pedogenic soil horizon down to 2 m or restrictive feature and  
187 analyzed for several properties including total soil carbon concentration, calcium carbonate concentration,  
188 bulk density, coarse fragments, soil pH, and texture. Soil organic carbon stocks used in CTSM were  
189 estimated for each soil horizon by calculating organic carbon concentrations (after subtracting carbonates  
190 from total carbon measurements) and multiplying by bulk density.

191 Currently, the CTSM simulations are run with a single plant functional type (PFT) at each NEON  
192 site (Table S1). We acknowledge that this belies the diversity in vegetation that is present at NEON sites,  
193 but it provides a tractable starting point for further investigation into developing more sophisticated site-  
194 regional-scale parameterizations and representations of biotic diversity with CTSM. CTSM represents  
195 mixed species communities as separate patches occupied single PFTs. CTSM can represent more than  
196 one PFT at each site, and users can update the provided CTSM surface dataset to include more than one  
197 PFT and future efforts may provide datasets with multiple PFTs corresponding to their proportion at  
198 NEON sites. The dominant PFT at each NEON site was assigned at the location of each EC tower using  
199 expert assessment that was informed by NEON vegetation surveys. Information on soil properties and  
200 dominant vegetation types are output as .csv files to public-access cloud storage buckets for use by  
201 CTSM (Figs. 1; Sect. 2.3).

202 *2.1.3 Independent model evaluation*

203 The EC flux data (energy, water vapor, and CO<sub>2</sub>) are time regularized and quality assurance and  
204 control (QA/QC) are applied. The QA/QC applied includes removing data when quality flags are raised,  
205 removing CO<sub>2</sub> data when the field calibration algorithm cannot be applied, applying range thresholds, and  
206 applying a despiking routine to remove outliers (Brock, 1986; Starkenburg et al. 2016). The data are gap-  
207 filled using the ReddyProc methodology outlined in Sect. 2.1.1. The vapor pressure deficit (VPD) is  
208 derived from the difference between actual and saturated vapor pressure, while gross primary production  
209 (GPP) is calculated from net ecosystem exchange (NEE), the sum of turbulent and storage fluxes, using  
210 the nighttime flux partitioning method of Reichstein et al. (2005). The nighttime approach is a community  
211 standard and was used at all sites in this work, and future work can explore whether other partitioning  
212 approaches may be more appropriate at some sites. The data, quality flags, and metadata are formatted  
213 and provided at 30-minute intervals as netCDF files for comparison with modeled fluxes. In future  
214 releases of the NCAR-NEON system we aim to use the ONEFlux data pipeline to enable additional  
215 methodologies for flux partitioning, which also includes storage fluxes (Pastorello et al. 2020). Finally,  
216 NEON continuous soil moisture data were compared with model simulations for two sites. Since the soil

217 moisture sensors were reconfigured with different calibration coefficients during the 2018-2021 validation  
218 period, which introduced step changes in NEON's soil moisture data product (Table 1), the raw sensor  
219 measurements were back-calculated and consistent soil-specific calibration coefficients were  
220 subsequently applied over the entire measurement period (Ayres et al. 2021) prior to comparison with  
221 CTSM data. Only values that passed quality tests were used. In future work we aim to provide  
222 standardized soil moisture data for more sites across the Observatory.

## 223 **2.2. NCAR modeling**

224 Numerical models of weather and climate have long been recognized as essential research tools  
225 to advance atmospheric science. Land surface fluxes of energy, moisture, and momentum, required to  
226 solve the equations of atmospheric physics and dynamics, are controlled by heat and water storage in  
227 soil, as well as the physiology of plants and their organization into canopies of leaves. Consequently,  
228 models of soil-plant-atmosphere processes are required to provide the necessary surface fluxes. Indeed,  
229 the first numerical weather prediction model included mathematical equations for soil temperature, soil  
230 moisture, the stomata on leaves, and envisioned canopies as a film of leaves covering the surface  
231 (Richardson 1922). As science progressed from models of atmospheric general circulation to climate  
232 models and now, Earth system models, the role of terrestrial ecosystems in climate processes has come  
233 to the forefront. The terrestrial components of ESMs, such as CTSM, have improved ecological processes  
234 representation and now include biogeochemical cycles, wildfires, and land use and land cover change  
235 (Bonan 2015, 2019; Lawrence et al. 2019). This evolution in the Earth system sciences is evident in 40+  
236 years of scientific research linking weather, climate, and land modeling at NCAR, from pioneering initial  
237 model implementations (Deardorff 1978; Dickinson et al. 1986, 1993; Bonan 1996) to community-based  
238 model development (Oleson et al. 2004, 2010, 2013; Levis et al. 2004; Lawrence et al. 2019) that  
239 continues to engage ecological and environmental sciences communities in CTSM development and  
240 application. As more ecology and biogeochemistry are added to the models (Fisher and Koven, 2020),  
241 the notion of climate prediction is expanding to Earth system prediction, including terrestrial ecosystems  
242 and biotic resources (Bonan and Doney 2018). These models have also become important tools for  
243 scientific discovery by identifying the ecological processes that affect climate (e.g., photosynthetic  
244 temperature acclimation; Lombardozzi et al. 2015) and to advance theory at the macroscale (e.g.,  
245 developing a theory of ecoclimatic teleconnections; Swann et al. 2018). With the new NCAR-NEON  
246 system tools described here, we aim to expand engagement and accessibility with the ecological and  
247 environmental sciences communities to continue testing, evaluating, and improving terrestrial process  
248 representation within CTSM. This will improve our understand of how ecosystems function within the  
249 Earth system, including the regulation of carbon, water, and energy fluxes that affect climate.

### 250 2.2.1 Containerized version of CESM-Lab

251 CESM has a long history of being freely and openly available to users (Hurrell et al. 2013;  
252 Danabasoglu et al. 2020), yet several barriers related to training, cyberinfrastructure, and data integration  
253 have hampered its adoption by a wide range of researchers. Even with open-source software, porting  
254 CESM to a new computer also requires the new computing system can compile model source code and  
255 has all the necessary input data and library dependencies. To address these computing challenges,  
256 NCAR recently developed CESM-Lab, which is a pre-configured and standardized environment that  
257 contains CESM and Jupyter-Lab. CESM-Lab is available via a Docker container and distributed via  
258 DockerHub (Table 2). The containerized version of CESM-Lab, and containers in general, give  
259 researchers the capability to package and distribute source code, libraries, dependencies, and system  
260 settings as one unit – thereby ensuring reproducibility. Using the containerized system, CESM-Lab can  
261 be used on any computing system, even a laptop or a cloud platform, to allow researchers to easily run  
262 CESM and its component models. The NCAR-NEON system uses CESM-Lab capabilities to run single  
263 point CTSM simulations at NEON sites.

### 264 2.2.2 Single point CTSM simulations

265 The workflow for running single-point CTSM simulations requires several steps that can be error-  
266 prone and time-consuming, particularly when using EC tower or other site-level data to drive simulations.  
267 To facilitate using NEON data in CTSM simulations we made several modifications to simplify this  
268 workflow. When users create a new simulation, the system queries NEON public-access cloud storage  
269 buckets and downloads available data into a designated directory (Sect. 2.3). For each NEON site, this  
270 includes a surface dataset that reflects soil properties and the dominant vegetation (Table 1),  
271 meteorological data that provide boundary conditions for the land model, and an initial conditions file with  
272 equilibrated, or steady-state, carbon, water, energy, and nitrogen states to initialize ecosystem pools  
273 simulated by CTSM. Initial conditions at each NEON site were generated by cycling over the  
274 meteorological data at each site for 200 years in accelerated decomposition (AD) mode and another 100  
275 years in normal, or post-AD mode, or until biogeochemical states reached steady state (when ecosystem  
276 C pools change by  $< 1 \text{ g C m}^{-2} \text{ y}^{-1}$ ; this is standard protocol for equilibrating the model state, Lawrence et  
277 al. 2019). Colder sites, especially those in Alaska, took longer to reach these steady state conditions.

278 The NCAR-NEON system uses a top-level Python code called 'run\_neon' that simplifies  
279 downloading the preconfigured datasets and automatically creates, builds, and runs cases for individual  
280 and multiple NEON sites. The Python script, which also resides in the CTSM repository (Table 2),  
281 includes several command-line arguments and options for automatically running spin-up and transient  
282 simulations. Collectively, these features dramatically improve CTSM site simulation accessibility, facilitate  
283 the use of new NEON data, reduce potential errors in configuring the CTSM case at NEON tower sites,  
284 and enable users to run simulations at multiple NEON sites. While users of the system can now easily  
285 generate their own data, NCAR provides model simulation data at each of the tower sites that are

286 available on the NEON public-access cloud storage bucket (Sect. 2.3). Simulation data are generated at  
287 a 30-minute time step and are aggregated into daily netCDF files.

### 288 *2.2.3 Tutorials, analysis, and visualization*

289 Three interactive tutorials are available to guide users through the new NCAR-NEON system  
290 (Table 2). The first tutorial helps system users to access CESM-Lab using Docker, which will ultimately  
291 allow the user to run CTSM simulations at NEON sites on their local computing system. The first step  
292 requires that users download Docker from the company website. This step is potentially challenging, as  
293 Docker is an externally controlled application and some recent Docker updates do not work with older  
294 computing systems. We provide links to additional resources to help the user navigate these potential  
295 problems and offer a resource for asking questions about containers through the CESM discussion forum  
296 (Table 2). After downloading and installing Docker, users are guided through downloading, running, and  
297 connecting to the CESM-Lab container and accessing the NEON tower simulation and visualization  
298 tutorials.

299 The second tutorial is a Jupyter Notebook that guides users through running CTSM simulations  
300 for NEON flux tower sites. The beginning of this tutorial provides a short description about CTSM and its  
301 component models, as well as resources for finding additional information. The process of running a  
302 simulation at NEON tower sites has been streamlined into the 'run\_neon' script (see Sect. 2.2.2) that can  
303 be called with a single line of code after the user defines a NEON tower site. The simulation itself  
304 downloads approximately 2.5 GB of input data and takes several minutes or more to complete, depending  
305 on the speed of the internet connection and computing system being used. After the simulation  
306 completes, the user is pointed to where the model data are stored and has the option to generate plots of  
307 soil temperature and moisture profiles for one year of the simulation.

308 The third tutorial guides users through analyzing and evaluating model simulations against  
309 observed NEON flux tower measurements. This tutorial requires a successfully completed NEON tower  
310 simulation from the previous simulation tutorial. The user selects their site and the year of interest and is  
311 guided through loading and opening the model data files, as well as downloading EC data for evaluation  
312 from the NEON server and loading and opening the files. Next, the tutorial guides users through  
313 formatting, processing, and plotting simulation and flux tower data. Users generate plots of mean annual  
314 and diel cycles of latent heat flux. Additional plots illustrate how CTSM partitions latent heat flux into  
315 ground evaporation, canopy evaporation, and transpiration, as component fluxes are not available from  
316 the observed data. Scatter plots are also created using simulated fluxes to illustrate the relationship  
317 between component evaporation and transpiration fluxes and total latent heat flux on seasonal and  
318 annual timescales. The tutorial explains the python tools used to process and plot the data and asks  
319 probing questions about the results that tutorial users are exploring to help guide the user in thinking  
320 about patterns in the data and consider how to compare model and flux tower data. Users are  
321 encouraged to use the code available in this tutorial to explore other sites, years, and variables.

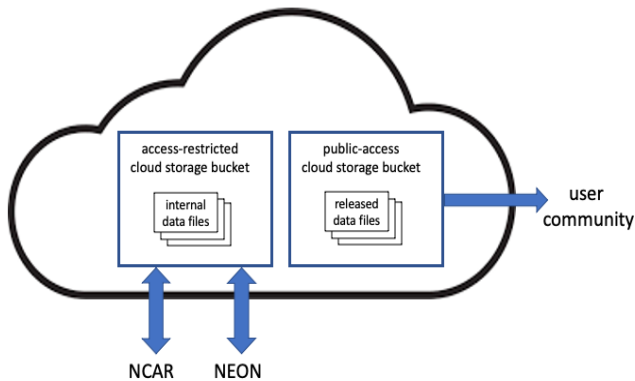


Figure 2. A schematic representation of the cloud-based data management for the NCAR-NEON system. Internal data may include preliminary results, data shared for review within the project, or data staged for release. Released data files are available for public access to the user community and anyone on the Internet and include NEON meteorological inputs, NEON surface characterization data, CTSM surface datasets and initial condition files, NEON measurements used for model evaluation, and data from CTSM simulations that are used for interactive visualizations. Access-restricted cloud buckets require authentication to access files stored in them. Public-access cloud storage buckets provide open access to the files stored in them.

### 2.3 Cyberinfrastructure to Facilitate Data Exchange and Interactive Visualizations

Cyberinfrastructure for scientific data provides data handling and management functionality including data storage, processing, transfer, security, and access. Cyberinfrastructure components developed for the NCAR-NEON system include access-managed cloud storage for project data, standards-based metadata generation enabling dataset search and discovery, and data exploration tools for the user community. Datasets for the NCAR-NEON system are hosted in cloud object storage providing secure web-enabled access to the data files (Fig. 2). Data files are grouped in the cloud storage system into logical storage containers called buckets. Buckets that are granted

340 public access allow anyone on the Internet to download the data stored in them. Buckets protected with  
 341 authentication mechanisms require users to have either individual account permissions on the bucket or  
 342 an access key for the bucket and are meant for internal dataset sharing or staging data prior to public  
 343 release.

344 Data exchange between NCAR and NEON within this system enables automated generation of  
 345 datasets as well as collation of NCAR model outputs and NEON data. The initial data collation for NEON  
 346 data products uses a container that sources all atmospheric forcing and model evaluation data from the  
 347 NEON API, performs gap-filling, and formats the data for model ingestion with standardized metadata  
 348 (Sect. 2.1). Simulation datasets from NCAR (Sect. 2.2) are automatically synced to NEON object storage  
 349 in the cloud at scheduled intervals (Fig. 2). To facilitate automated transfer of datasets between NCAR  
 350 and NEON, a staging bucket is configured that allows file uploads from authenticated users. An  
 351 automated process moves files from the staging bucket to the publicly available target bucket at  
 352 scheduled intervals. Metadata describing scientific datasets using standard vocabularies and formatting  
 353 can be used by Internet search engines to facilitate dataset discovery. JavaScript Object Notation for  
 354 Linked Data (JSON-LD; <https://www.w3.org/TR/json-ld>) is a human- and machine-readable open  
 355 metadata standard. Schema.org defines a vocabulary of standard HTML tags compatible with JSON-LD  
 356 markup (Shepherd et al. 2022). A metadata generation component for NCAR-NEON datasets is  
 357 implemented in Python and uses the Binary Array Linked Data library (binary-array-ld 2016) to generate  
 358 JSON-LD metadata for NCAR-NEON netCDF files with the Schema.org vocabulary.

359           Beyond these automated data exchanges, we also developed a Python-based interactive  
360 visualization dashboard (Table 2) as a Graphical User Interface (GUI) that enables users to explore and  
361 interact with model outputs and observations on-the-fly. This tool allows users to generate graphs and  
362 statistical summaries comparing CTSM simulations and observational data for NEON sites without  
363 downloading the observational data or running the model. This dashboard was developed using a  
364 scientific Python stack, including Xarray, Bokeh, and Holoviews, which allows a developer to create a  
365 user interface with widgets and visualization components inside a Jupyter Notebook. Users access a GUI  
366 to select individual NEON sites, variables, and output frequencies to visualize. The tool offers different  
367 types of interactive visualizations and statistical summaries based on users' selections. This interactive  
368 visualization dashboard does not require specialist knowledge to operate; therefore, it can be used for  
369 educational outreach activities and in classrooms. Moreover, users can interact with the dashboard using  
370 a browser, so it is possible to interact with the plots via tablet or smartphone.

371           Data input-output and manipulation, particularly at the 30-minute frequency available in the  
372 NCAR-NEON system, are typically computationally resource-intensive aspects of data access. Input-  
373 output and calculations can both benefit from parallel computing, which can process multiple subsets of a  
374 dataset simultaneously and thereby enable efficient dataset access and operations. The back end for the  
375 visualization dashboard uses dataset chunking for efficient access to netCDF file content. The Zarr format  
376 and library enable generation of metadata providing chunked access to netCDF files (Miles et al. 2022).  
377 Zarr metadata for daily files is combined into monthly files, reducing the number of files accessed for time  
378 intervals spanning multiple days and thereby improving access efficiency. The Python Xarray library,  
379 which is used to read the datasets, integrates with the Python Dask library for parallel computing and thus  
380 enables loading and processing netCDF data chunks in parallel as Dask arrays. The Dask components  
381 that Xarray uses use a local thread pool by default, and local threads incur minimal task overhead  
382 associated with the parallel processing. Operations on the Dask arrays use the Python NumPy library for  
383 array operations, and the NumPy implementation takes advantage of thread pool parallelism, enabling  
384 efficiency improvements in dataset operations even on small (~100-200 KB) files.

### 385 **3. Results**

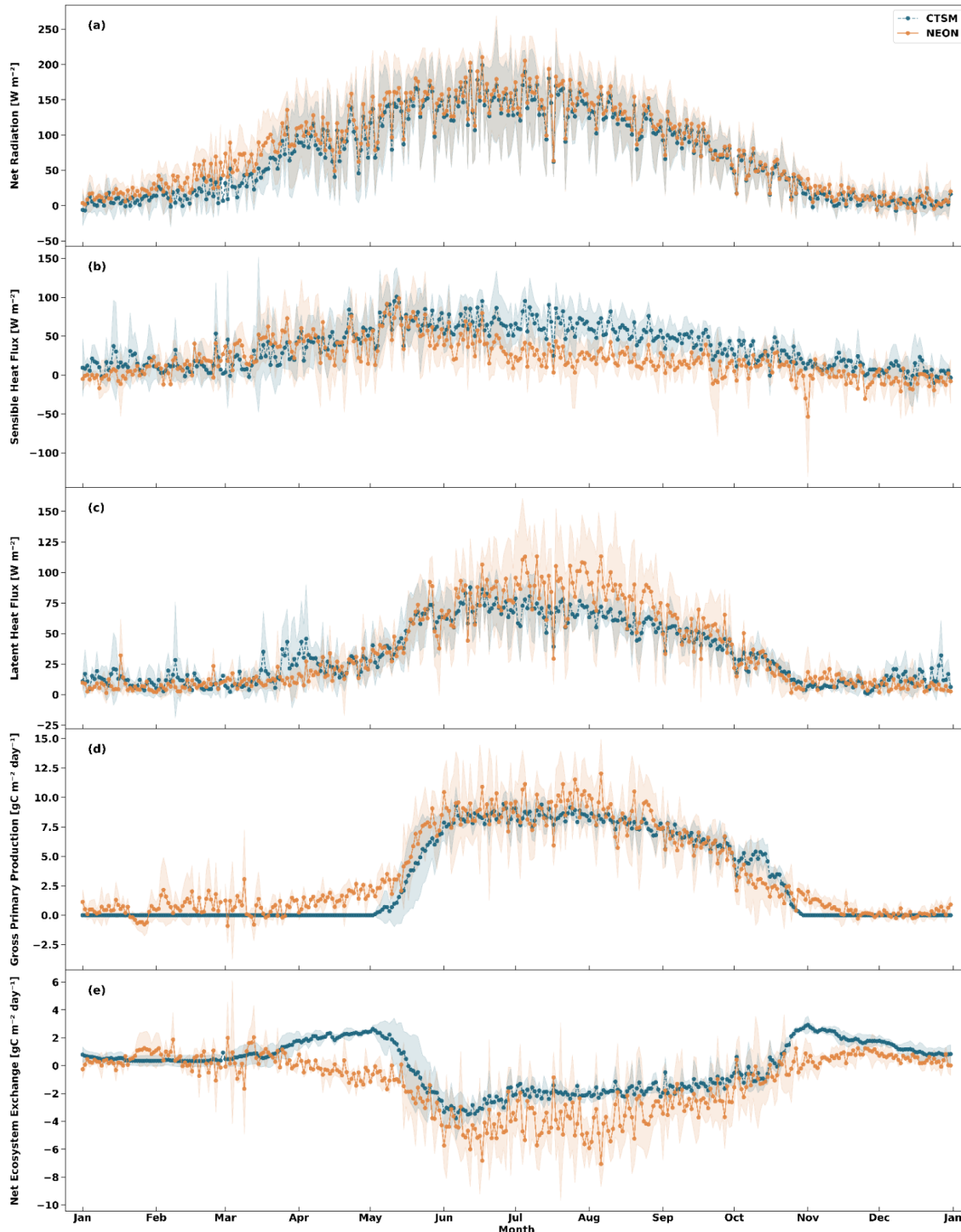
386           We illustrate features of the NCAR-NEON system with comparisons of observed and simulated  
387 fluxes across diverse ecosystems that the Observatory spans. A subset of the sites highlighted in our  
388 analysis are described in Table 3. The comparisons are intended to summarize the status of the project,  
389 illustrate the data produced through this project, and highlight potential insights the data affords. We  
390 recognize that there are rich opportunities to expand on these analyses, integrate additional  
391 measurements, and improve modeled parameterization and representations of specific sites and  
392 processes. Indeed, such contributions are encouraged from the community.

393

394 **Table 3** Summary of site name, location, mean annual temperature (MAT), mean annual precipitation (MAP), gross  
 395 primary production (GPP) and latent heat flux at a subset of NEON sites. Values show annual means and standard  
 396 deviations in parentheses. Due to gaps in the NEON observational estimates, mean annual GPP and latent heat fluxes  
 397 are for the full time series simulated by CTSM at each site. All results are for 2018-2021 unless noted otherwise. The  
 398 full list of results is shown in Tables S1, S2.

NEON Site ID	Site Name	Lat	Lon	MAT (°C)	MAP (mm y <sup>-1</sup> )	GPP (g C m <sup>-2</sup> y <sup>-1</sup> )	Latent Heat (W m <sup>-2</sup> )
BART	Bartlett Experimental Forest	44.065	-71.2883	7.7 (0.7)	1213 (146)	1126 (57)	33.6 (1.3)
HARV	Harvard Forest	42.536	-72.1756	8.5 (0.6)	1404 (502)	1153 (53)	32.3 (1.8)
STEI	Steigerwaldt-Chequamegon	45.508	-89.5888	5.7 (0.9)	659 (110)	1109 (88)	29.7 (0.8)
KONZ	Konza Prairie Biological Station	39.101	-96.5623	12.9 (0.7)	617 (168)	1158 (235)	49 (4.8)
SRER	Santa Rita Experimental Range	31.911	-110.835	20.4 (0.7)	328 (104)	360 (133)	26.1 (6.8)
ABBY	Abby Road	45.762	-122.33	10.1 (0.4)	2042 (409)	1906 (35)	29.5 (1.3)

399  
 400 Annual climatologies of site level data provide comparisons of measured and simulated fluxes.  
 401 Site level simulations with CTSM received inputs of incoming shortwave and longwave radiation  
 402 measured at NEON EC towers (Table 1), but the model calculates reflected shortwave radiation and  
 403 outgoing longwave radiation based on albedo and surface temperature. Accordingly, net radiation is a  
 404 useful metric by which to compare observed and simulated fluxes. Since net radiation is a driver of  
 405 numerous ecosystem fluxes, identifying biases can help to explain biases in other fluxes. We look at a  
 406 climatology of daily mean net radiation that is simulated over the NEON record. Results shown here for  
 407 Bartlett Experimental Forest (BART; Fig. 3a) suggest that the model adequately captures the seasonal  
 408 cycle of net radiation at this temperate deciduous forest site. (Fig. S1 shows a similar climatology for a  
 409 boreal forest site at Delta Junction (DEJU) in central Alaska).



410  
 411 **Figure 3** Climatology of daily mean NEON measurements (orange) and CTSM simulations (blue) at the Bartlett  
 412 Experimental Forest in New Hampshire (BART). Points show the daily mean (a) net radiation; (b) sensible heat flux;  
 413 (c) latent heat flux; (d) gross primary production (GPP); and (e) net ecosystem exchange (NEE). Shading shows the  
 414 standard deviation of daily average data for 2018-2021.

415

416 Users can also compare latent and sensible heat fluxes that are simulated by the model and  
 417 observed at EC towers. At BART we see that CTSM tends to overestimate sensible heat fluxes, while

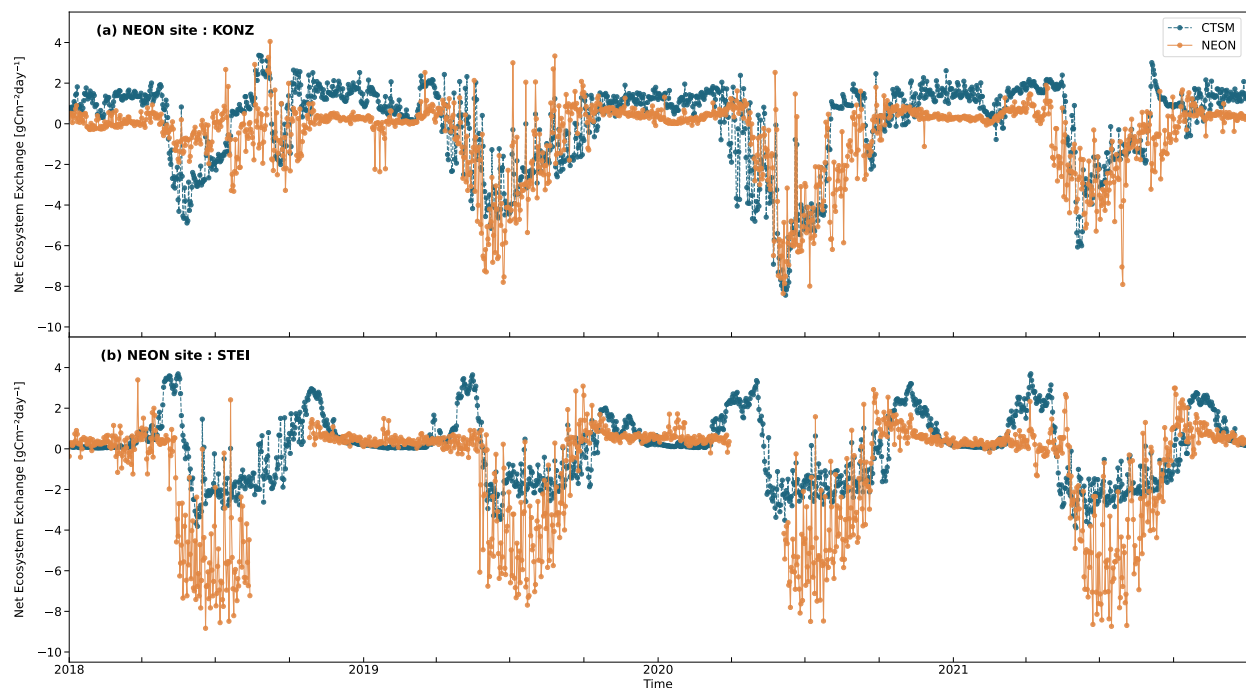


418 underestimating latent heat fluxes, especially during the summer months (Fig. 3b-c). Such biases in the  
419 evaporative fraction (the ratio of latent heat flux to the sum of latent and sensible heat fluxes) of turbulent  
420 fluxes are common in land models, including CTSM (Best et al. 2015; Wieder et al. 2017) and the NCAR-  
421 NEON system. The inconsistencies at BART could reflect model biases in stomatal conductance or leaf  
422 area index (LAI) and deserves further investigation. Future work can leverage data from PhenoCam data  
423 (Richardson et al. 2018) and stable isotope measurements at NEON towers (Finkenbiner et al. 2022;  
424 Moon et al. 2022) to better understand LAI and stomatal conductance, respectively.

425 Comparing measured and simulated carbon fluxes provides insights into model parameterizations  
426 and can be used to estimate missing observational data. Carbon fluxes from CTSM simulations can be  
427 compared to data from NEON EC towers: Net ecosystem exchange (NEE) data are measured at the  
428 NEON EC towers while GPP is a modeled product that is derived from statistical relationships, here using  
429 the nighttime flux partitioning method of Reichstein et al. (2005). By contrast, models like CTSM first  
430 simulate GPP based on leaf level photosynthetic rates that are scaled to the canopy with simulated LAI.  
431 Subsequently, NEE is calculated after subtracting ecosystem respiration fluxes from GPP. Results at  
432 BART suggest that CTSM generally captures the timing and magnitude of GPP fluxes at the site (Fig. 3d);  
433 although attention to phenology, especially environmental controls and interannual variability of leaf out  
434 and senescence are likely warranted (Birch et al. 2021; Li et al. 2022). The climatology of NEE fluxes  
435 simulated by CTSM shows biases during the spring and autumn when the model simulated a land source  
436 of CO<sub>2</sub> to the atmosphere (Fig. 3e) due to high ecosystem respiration fluxes. Moreover, the land sink of  
437 CO<sub>2</sub> in the summer appears to be weaker in CTSM simulations than the NEON observations at the BART  
438 tower (Fig. 3e). Since the magnitude of GPP is similar in the model and observations, the underestimated  
439 summer NEE is possibly due to high biases in simulated ecosystem respiration fluxes. Diagnosing the  
440 source of this model biases is challenging, in part due to the interconnectivity of simulated processes and  
441 the limited capacity to measure such processes. Deeper insights may be afforded by taking a closer look  
442 at results with higher temporal frequencies.

443 NEON tower data are simulated in near-real time within the NCAR-NEON system, with data  
444 available to simulate most towers starting in 2018 through the most recent full year, here 2021. Figure 4  
445 shows daily mean carbon fluxes, NEE, that are measured and simulated for the Konza Prairie Biological  
446 Station (KONZ), where the NEON tower is in an unplowed tallgrass prairie in Kansas, and Steigerwaldt  
447 Land Services (STEI) site, where the NEON tower is located in an early successional aspen stand in  
448 Wisconsin. Positive NEE fluxes show net carbon release from land to the atmosphere, while negative  
449 fluxes indicate carbon gain into ecosystems. Looking at the full data record shows several notable  
450 features of NEON measurements and CTSM simulations. Data gaps in NEON measurements are most  
451 common during the early operation of the observatory (Aug-Oct of 2018 at STEI) and in the early months  
452 of the COVID-19 pandemic, when field crews could not travel to field sites to maintain equipment (Apr-  
453 June of 2020 at STEI). Across the observatory the NEON EC measurements have greater than 70% data  
454 coverage, up from less than 40% data coverage at the start of observatory operations. The current NEON

455 EC data coverage aligns with that of the FLUXNET2015 dataset (van der Horst 2019). Second, although  
456 EC is directly measuring NEE, mean daily NEON observations show high variability at both sites. Finally,  
457 NEON EC towers measure both storage and turbulent fluxes, but results shown here omit the storage  
458 component. Storage fluxes contribute to uncertainty in measured NEE fluxes, which may (or not) be large  
459 for individual sites at different times of year.  
460

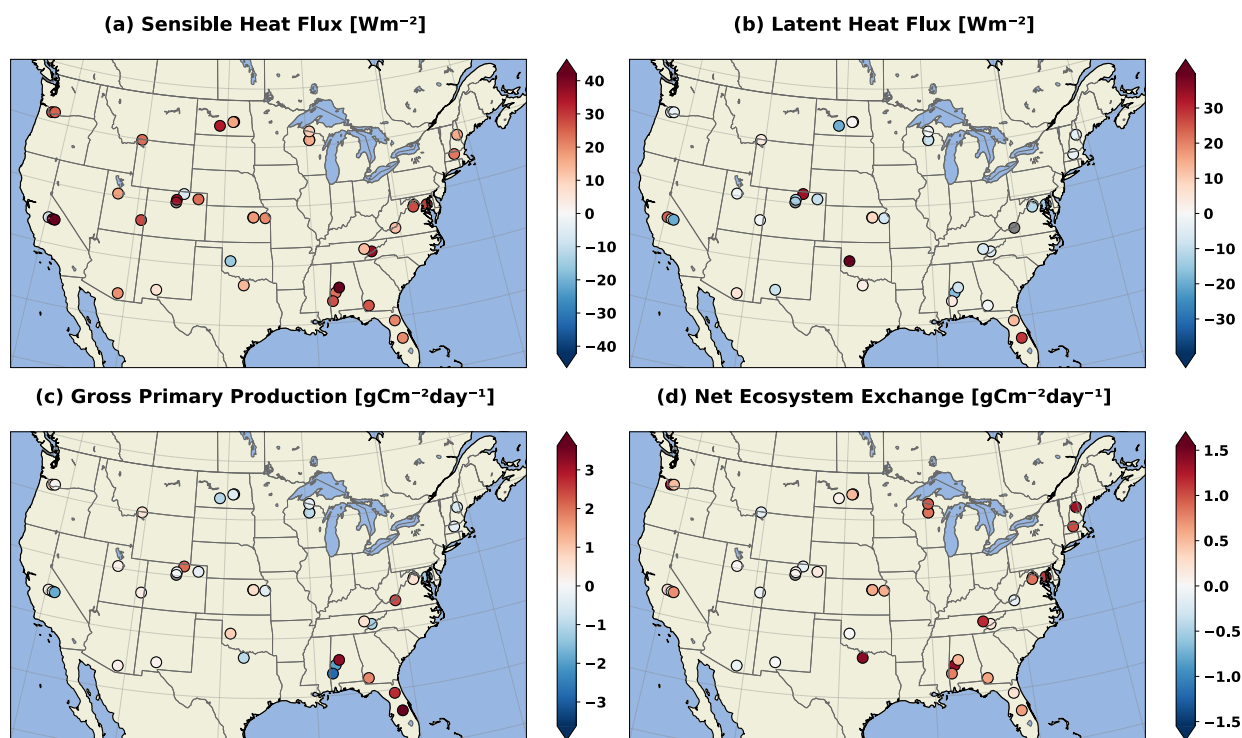


461  
462 **Figure 4** Full time series of daily mean net ecosystem exchange (NEE) from NEON measurements (orange) and CTSM  
463 simulations (blue) at the (a) Konza Prairie Biological Station in Kansas (KONZ) and (b) Steigerwaldt Land Services site  
464 in Wisconsin (STEI). Positive NEE fluxes show net carbon release from land to the atmosphere, while negative fluxes  
465 indicate carbon gain into ecosystems.

466  
467 The NEE fluxes that are simulated by CTSM are calculated as the differences in GPP and  
468 ecosystem respiration fluxes, which includes both autotrophic and heterotrophic respiration. These  
469 component fluxes are much larger, depend on simulated ecosystem states (LAI, vegetation biomass, and  
470 soil organic carbon stocks) and have associated environmental sensitivities (e.g., temperature,  
471 precipitation, etc.). Thus, biases in these component fluxes can potentially transmit biases to simulated  
472 NEE fluxes (Figs. 3-4). For example, CTSM simulations show periods of positive NEE during the spring  
473 and fall that are not evident in NEON observations. The seasonal biases in NEE could result from an  
474 underestimation of GPP during the shoulder season caused by phenological mismatches in simulated  
475 and observed LAI, or result from only simulating a single plant functional type in CTSM. Alternatively,  
476 NEE biases could result from higher than observed soil respiration rates in the model that reflect potential  
477 biases in total soil C stocks or the temperature sensitivity of heterotrophic respiration. Finally, the CTSM  
478 simulations were equilibrated to steady state conditions, meaning that annual NEE averaged over the  
479 simulation period will be zero. The real ecosystems being measured at NEON sites, however, have

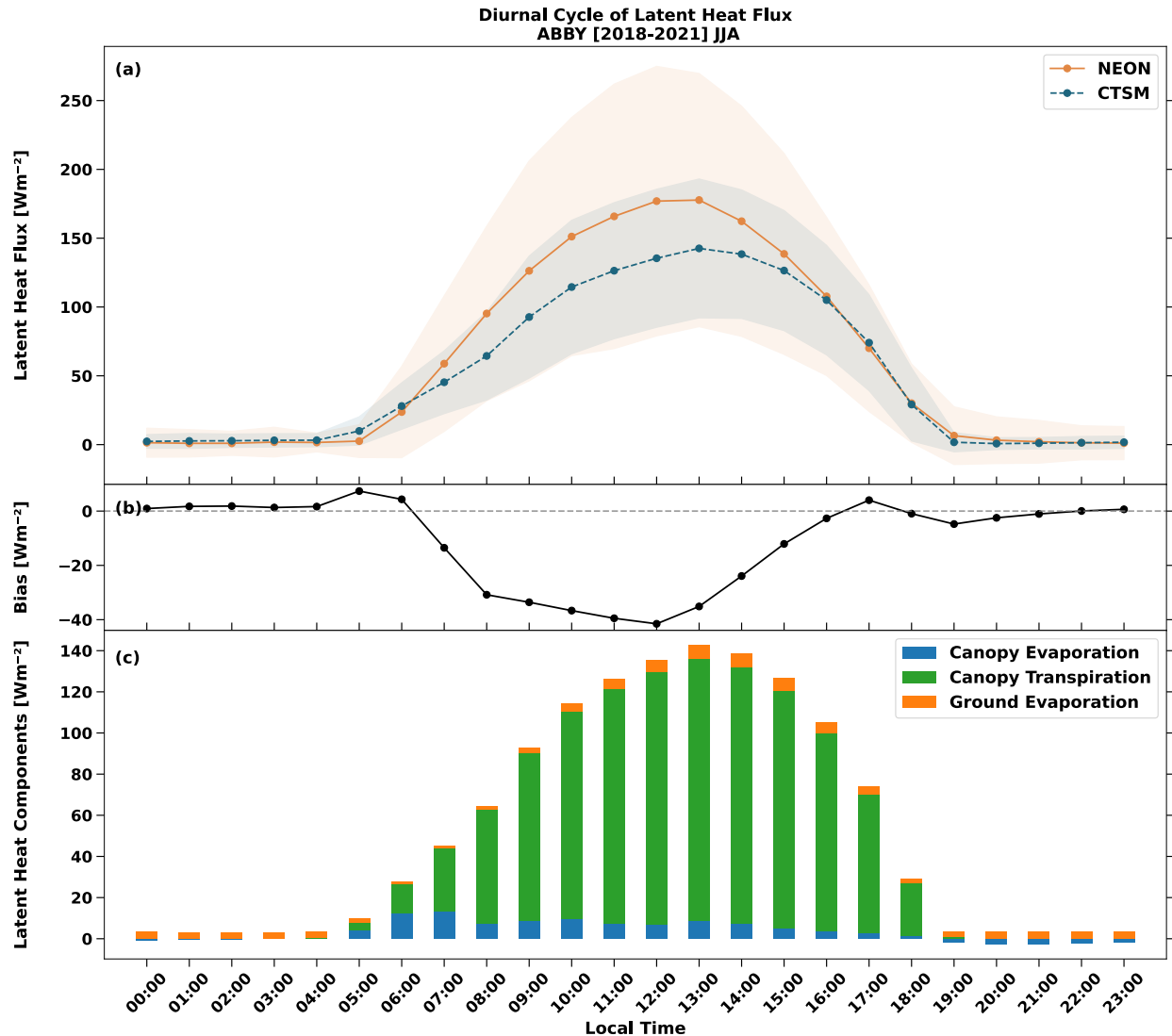
480 historical legacies – KONZ is burned periodically and STEI is an aggrading forest site – and do not  
 481 necessarily meet these same steady state assumptions. Collectively, this points to rich opportunities to  
 482 learn about the ecosystems being measured by NEON observations and the processes that are important  
 483 to represent in models like CTSM.

484 We calculated summary statistics of CTSM simulated bias (Fig. 5) and root mean square error  
 485 (RMSE; Fig. S2) in ecosystem fluxes, compared to NEON observations. Biases in GPP and NEE are  
 486 relatively low in the Great Plains and Intermountain West but are larger in the Eastern US. Specifically,  
 487 NEE is biased high east of the Mississippi, while GPP biases are largest in the Southeastern US. CTSM  
 488 typically has high biases in sensible heat fluxes and concurrent low biases in latent heat flux. Some sites,  
 489 particularly grasslands (e.g., CPER, OAES, and SJER), do not follow this general pattern. We therefore  
 490 probed precipitation data from NEON, which appear to have significant biases at some grassland sites  
 491 (discussed in Sect. 4.1) and contribute to artificially high biases in CTSM simulations at these sites.  
 492



493 **Figure 5** Maps showing location of NEON site in the conterminous United States and annual biases in fluxes that are  
 494 simulated by CTSM for: (a) sensible heat flux ( $W m^{-2}$ ); (b) latent heat flux ( $W m^{-2}$ ); (c) gross primary production (GPP,  
 495  $gC m^{-2} day^{-1}$ ); and net ecosystem exchange (NEE,  $gC m^{-2} day^{-1}$ ) over the observational record (2018-2021), unless  
 496 otherwise noted in Table S2.  
 497

498  
 499 Additional insights into potential sources of biases in data-model comparisons can be provided by  
 500 looking deeper into component fluxes of latent heat at higher temporal frequencies. The NEON EC towers  
 501 provide 30-minute measurements of total latent heat fluxes, but latent heat fluxes in CTSM can be  
 502 partitioned into contributions from canopy transpiration, canopy evaporation, and soil evaporation. For

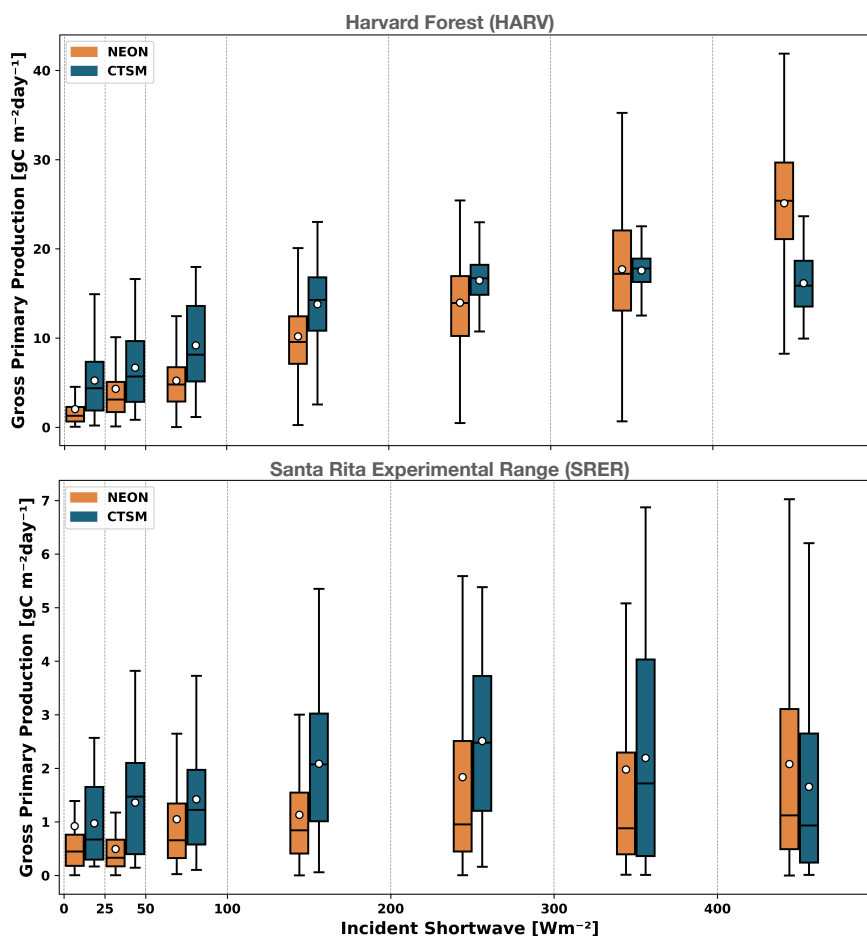


503  
 504 **Figure 6** Diel cycle of summertime (June, July, and August, or JJA) latent heat flux at the Abby Road site in Washington  
 505 (ABBY). Panels show: (a) mean half hourly fluxes (2018-2021 mean  $\pm 1\sigma$ ) for NEON measurements and CTSM  
 506 simulations (orange and blue lines, respectively); (b) CTSM model bias relative to the observations ( $W m^{-2}$ ); and (c)  
 507 partitioning of latent heat into fluxes that are simulated by CTSM, which includes canopy evaporation, canopy  
 508 transpiration, and ground evaporation (blue, green, and orange bars, respectively). Additional visualizations showing  
 509 all sites and seasons are available on the interactive visualizations web site (Table 2).

510

511 example, the CTSM simulations show temporal biases in both the timing and magnitude of mean diel  
 512 cycle of summertime (June, July, and August, or JJA) latent heat fluxes at the NEON Abby Road site  
 513 (ABBY; Fig. 6). The bulk of daytime latent heat fluxes simulated by the model are coming from canopy  
 514 transpiration fluxes, suggesting that the representation of stomatal conductance does not respond  
 515 correctly to atmospheric conditions or plant water availability. We also note that this site experienced two  
 516 very strong heatwaves in the summers of 2020 and 2021. Additional measurements of soil moisture, LAI,  
 517 or sap flux could help test, evaluate, and improve various model parameter values and parameterizations  
 518 to produce results that are most consistent with observed fluxes.

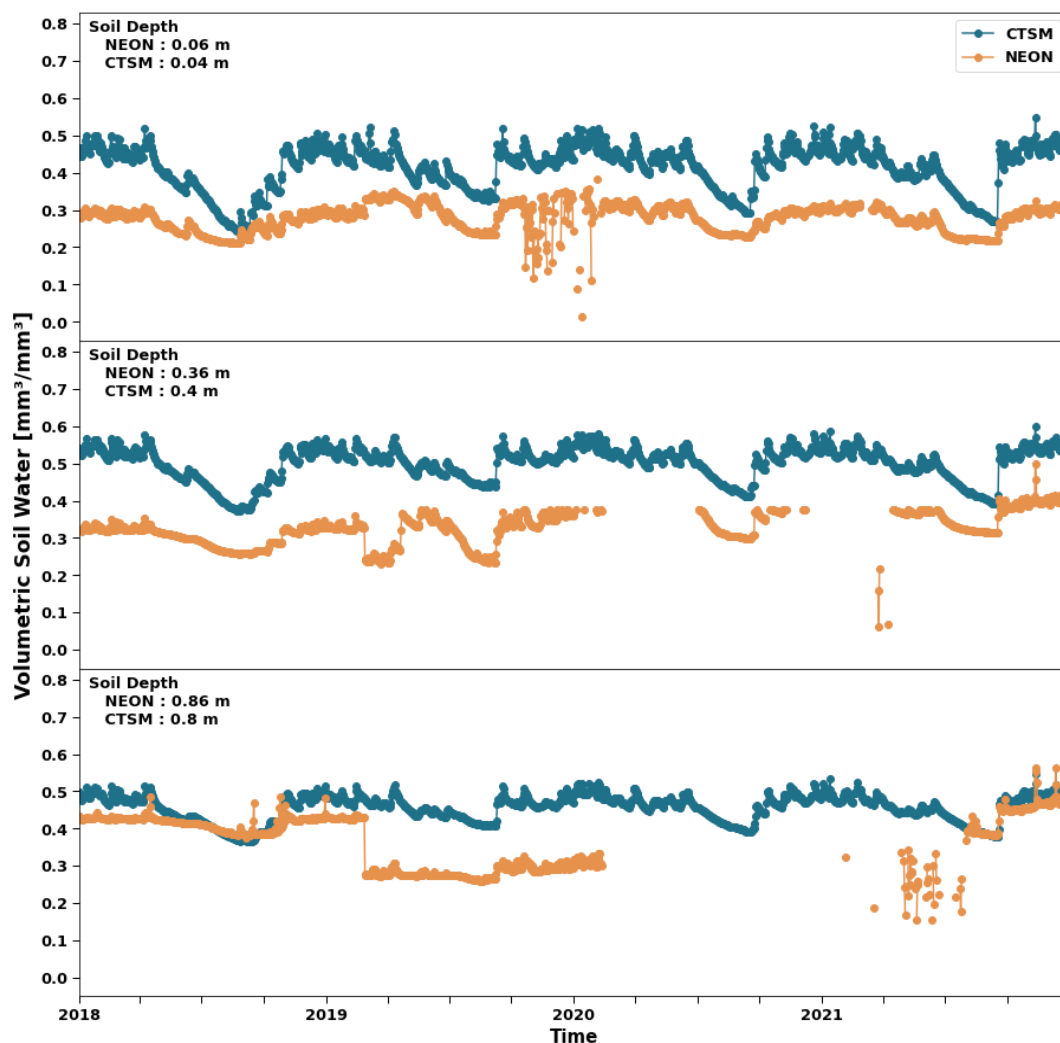
519 Light response curves (Fig. 7) illustrate how canopy photosynthesis responds to changes in the  
 520 radiation environment. At forested sites, CTSM tends to overestimate GPP at low light levels,  
 521 underestimate GPP under full irradiance and simulate lower variance in GPP across a range of high  
 522 incident radiation; this pattern is illustrated in Fig. 7a for Harvard Forest. At the Santa Rita grassland site,  
 523 GPP is biased high in most irradiance bins, although is comparable to observed estimates of GPP at full  
 524 irradiance (Fig. 7b). As GPP is the driver for carbon fluxes and plant-mediated water fluxes in CTSM,  
 525 inaccurate responses to light environment affects several processes, including NEE and transpiration,  
 526 which is a primary driver of mid-day (Fig. 6c) and summertime latent heat flux.  
 527



528  
 529 **Figure 7** Box-whisker plots showing light response curves, the relationship between gross primary production (GPP)  
 530 and incident shortwave radiation, that are derived from NEON measurements and CTSM simulations (orange and blue,  
 531 respectively) at (a) Harvard Forest (HARV) and the (b) Santa Rita Experimental Range (SRER). Data represent 30-  
 532 minute measurements that are binned by incident shortwave radiation levels observed at NEON sites over the  
 533 observational record in July (2018-2021). Boxes show the mean (dots), median (line), interquartile range (boxes). The  
 534 whiskers extend from the boxes (showing first and third quartiles) by 1.5 times the interquartile range (Q3-Q1). Note  
 535 differences in the scale of the y-axis.

536  
 537 Finally, there are opportunities to use data from CTSM simulations to augment NEON  
 538 measurements. For example, measurements of soil moisture are important for calculating soil CO<sub>2</sub> fluxes

539 from NEON sites, but the soil moisture probes currently deployed at NEON sites do not always provide  
 540 reliable measurements. For example, at the Abby Road site soil moisture observations have phases of  
 541 erratic measurements, are missing at depth throughout much of 2020 and 2021, and have large offsets  
 542 when instruments were calibrated (Fig. 8, Fig. S3). By contrast, CTSM provides continuous datasets that  
 543 could be used to gap fill or augment ongoing NEON soil moisture measurements, although simulated  
 544 data may need to be bias corrected. Similarly, soil moisture controls aspects of plant phenology in CLM,  
 545 meaning that soil moisture measurements could help constrain or explain potential biases in simulated  
 546 LAI and ecosystem fluxes. At ABBY, both CTSM simulations and NEON observations show similar  
 547 temporal patterns – a dry-down of soil moisture during the dry summer months and followed by wetter fall  
 548 winter and spring months (Fig. 8; Fig. S3), although CTSM simulates wetter soils than observed at the  
 549 NEON site.  
 550



551  
 552 **Figure 8** Time series of volumetric soil moisture profiles that are simulated by CTSM simulations (blue) and  
 553 measured by NEON (orange) at different depths in soil plot 3 at the Abby Road site in Washington (ABBY) from  
 554 2018-2021.

## 555 **4. Discussion**

556           The NCAR-NEON system links models and measurements to provide a powerful suite of tools to  
557 understand ecosystem properties and processes through space and time. In addition to facilitating the  
558 integration of measurements and modeling, a major focus of this work is to enable new opportunities for  
559 research and education by expanding access to and interaction with NCAR models and NEON data,  
560 contributing to a growing body of work that increases the accessibility and usability of large datasets and  
561 computing resources for research (e.g., Novick et al. 2018, Beringer et al 2020, Keetz et al. 2023) and  
562 education (e.g., Carey et al. 2020, O'Reilly et al. 2017). The user community can access quality-  
563 controlled and gap-filled NEON meteorological and EC flux data as prototype datasets through the public-  
564 access cloud storage buckets that supports the NCAR-NEON system or the Prototype Data section of the  
565 NEON Data Portal (Table 2). Additionally, the NCAR-NEON system streamlines running NCAR's CTSM  
566 model and simplifies access through the containerized CESM-Lab platform, bypassing the logistical  
567 challenges of porting CTSM to different computing systems. It also creates customized model input data  
568 that include local site characterizations of soil and vegetation using NEON data products, and allows  
569 users to add custom input data to simulate other locations. These capabilities allow researchers to focus  
570 their time on customizing CTSM and integrating additional NEON datasets to address research  
571 questions. Combined with the visualization software provided in the tutorials, the NCAR-NEON system  
572 also facilitates opportunities for teaching about land-atmosphere interactions, ecology, and land modeling  
573 and can be incorporated into undergraduate and graduate courses alongside similar efforts (e.g., Carey  
574 et al. 2015). Below we discuss some of the synergistic enhancements this collaboration makes for NEON  
575 measurements and NCAR models as well as opportunities that the NCAR-NEON system enables for  
576 research and teaching.

### 577 **4.1 Synergistic enhancements of NEON measurements and NCAR models**

578           The NCAR-NEON system is a collaborative partnership between observationalists and modelers  
579 that enhances both NEON's measurements and NCAR's models. One typically thinks of observations as  
580 improving models, but the reverse can also happen in which models inform and augment the collection of  
581 measurements. For example, models require continuous meteorological input data, so gap filling the  
582 missing meteorological data required to run CTSM was paramount to the success of the project. A new  
583 prototype data product provided by the project is a continuous time series of meteorological data at each  
584 NEON location. Comparison of modeled and measured EC fluxes identified QA/QC improvements to the  
585 meteorological data needed for the model simulations, and similarly improvements to the processing of  
586 the raw EC fluxes to compare with model results.

587           One issue raised in the simulations is the estimation of precipitation at grassland sites. NEON has  
588 experienced issues where small amounts of noise in the raw data cause spurious trace precipitation to be  
589 recorded at all primary precipitation sensors. Because secondary and throughfall precipitation buckets are

590 unaffected, there is a redundant data stream at forested sites, but these are unavailable for grassland  
591 sites. An updated algorithm is expected to resolve the spurious trace precipitation issue in late 2022 with  
592 back processed data available in the NEON 2024 data release. In the meantime, we manually evaluated  
593 the mean annual precipitation recorded at each NEON site against other observational data networks and  
594 noted locations where this issue is generating unexpectedly high or low precipitation values (Table S2).

595 Another example of how NCAR modeling improved NEON data quality comes from unusual soil  
596 moisture profiles that were initially generated in preliminary simulations at the ABBY site (data not  
597 shown). Upon closer inspection these patterns were found to be caused by an unusual relationship  
598 between soil organic carbon content and depth at this site, which did not match related data gathered  
599 during sample collection or subsequent analyses. Further investigation confirmed that the labels for the  
600 soil carbon analysis subsamples had been switched for two ABBY soil horizons. The NEON soil data  
601 have since been corrected and the modeled soil moisture profiles for ABBY now follow a more typical  
602 pattern with surface soils drying out during the summer and less variation in soil moisture in deeper soil  
603 horizons (Figs. 8, S3). There are also important differences in vertical profiles of simulated and measured  
604 soil moisture, with soil moisture simulated by CTSM typically decreasing with depth while NEON soil  
605 moisture observations generally increase with depth. Additional investigation is needed to determine if  
606 these discrepancies extend to other sites and indicate issues with CTSM simulations or NEON data  
607 products, but it does underscore a synergy in NCAR modeling and NEON measurements that deserves  
608 more attention moving forward.

609 We see clear opportunities for NEON observations to help guide future model improvements,  
610 especially related to potential biases in phenology (discussed above), photosynthesis (Fig. 7), and other  
611 processes. Some biases in modeled processes are already documented; for example, Wozniak (2020)  
612 found that CTSM underestimates maximum rates of simulated GPP compared to EC observations in  
613 deciduous forest sites. This suggests that implementation of the photosynthesis scheme in CTSM has  
614 parametric or structural issues that prevent high rates of GPP from occurring in the model. Auxiliary data  
615 from NEON that are not always available from other EC flux towers, for example foliar chemistry, can be  
616 used to update parameter values and to evaluate correlated model variables and processes. The  
617 opportunities afforded by NEON's EC and auxiliary data to improve the representation of ecological  
618 processes in CTSM will improve modeled carbon fluxes at NEON towers and may also ameliorate biases  
619 in global simulations.

620 Finally, the NCAR-NEON system can also facilitate model-informed prioritization of future data  
621 collection efforts. Models can quantify the dominant drivers of uncertainty in model parameters as well as  
622 in response to environmental drivers using ensemble-based methods of parameter uncertainty  
623 propagation and variance decomposition (LeBauer et al. 2013). Site-level CTSM simulations could  
624 therefore help future NEON data collection campaigns to target variables that contribute the most to  
625 uncertainty in modeled ecosystem fluxes and ecosystem responses to global change.



## 626 **4.2 Opportunities enabled for research**

627 The NCAR-NEON system enables research opportunities in the ecology, global change, and  
628 Earth system science communities by: (1) Facilitating access to NCAR models that can be customized to  
629 meet researchers' needs; (2) Providing a computational platform that leverages NEON observational  
630 datasets for site-level model configuration and evaluation across the diverse range of ecosystems  
631 captured in the NEON design; (3) Facilitating reproducible research workflows; and (4) Providing gap-  
632 filled meteorological data and partitioned EC flux data products that create synergies with other flux  
633 networks and data pipelines (Novick et al. 2018, Beringer et al. 2020, Pastorello et al. 2020).

634 In building the NCAR-NEON system we improved the software infrastructure and workflows that  
635 are required to run single point simulations with CTSM, while developing derived, prototype datasets with  
636 NEON's EC measurements. Although the focus of this work is on connecting CTSM and NEON data,  
637 measurements from non-NEON sites can also be used with this system, facilitating the use of data from  
638 additional EC towers and the ONEFlux data pipeline in CTSM development and evaluation. Moving  
639 forward, NEON is working with Ameriflux to incorporate the redundant data stream gap-filling from NCAR-  
640 NEON with ONEFlux standardized data processing as well as providing proper data formats and  
641 metadata for modeling framework ingestion.

642 Through CESM-Lab, the NCAR-NEON system provides access to the full model code and  
643 datasets used to run CTSM on any computing system. A strength of this system is the auxiliary data  
644 collected by the NEON network that is used to inform site-specific model inputs and model evaluation.  
645 With some effort, users can adapt this system to incorporate and simulate flux towers at other research  
646 sites using the 'Processing NEON data' tools linked in Table 2 to guide data formatting. Thus, future work  
647 could expand this system to include gap-filled flux data from other regional and global networks like  
648 AmeriFlux and FLUXNET, allowing for broader spatial coverage. Additionally, researchers do not need  
649 access to large-scale computing resources and can use alternative model configurations; the CTSM code  
650 can be modified and compiled within the container, so researchers who wish to run simulations with new  
651 model parameterizations or with additional model features may now do so from any computer. Most  
652 personal laptop computers are more than sufficient for running site level simulations, even when using  
653 more computationally complex versions of the land model that include, for example, ecological dynamics  
654 (using the Functionally Assembled Terrestrial Ecosystem Simulator, FATES; Koven et al. 2020) or  
655 representative hillslope hydrology (Swenson et al. 2019). Advanced users can run CTSM at any single  
656 point site by making their own input files. Additionally, researchers can quantify the impact of adjusting  
657 model parameters and processes on terrestrial ecosystems under historical and future climate scenarios.  
658 This flexibility is useful for calibrating the model to improve model performance at a given site, as well as  
659 for gaining mechanistic insights into how different processes and uncertainties affect ecosystem  
660 functioning. Broadening access to CTSM also allows researchers to rapidly compare model output to their  
661 own observational datasets, or to existing NEON observational datasets that are not yet integrated into  
662 the NCAR-NEON system.

663 Moving forward, we see additional NEON data products as providing valuable insights to the  
664 NCAR-NEON system. These could include NEON measurements that are used both as model inputs  
665 (foliar chemistry, phenology and LAI, and historical land use legacies) and as model validation datasets  
666 (including snow depth, vertical profiles of canopy temperature, leaf water potential, litterfall rates, biomass  
667 and vegetation structure, and depth profiles of soil moisture, temperature, carbon and nitrogen). Although  
668 these data have not yet been integrated into the NCAR-NEON system, we are optimistic that existing  
669 tools can help facilitate their integration into research opportunities. We see powerful opportunities to  
670 expand on this approach to integrate information from NEON's Airborne Observation Platform (AOP) into  
671 workflows that extend model capabilities beyond the relatively small footprint of the EC towers. For  
672 example, the AOP light detection and ranging (LiDAR) data would provide information to initialize stand  
673 structure that would be helpful for calibrating reduced complexity configurations of the CTSM-FATES  
674 model (Fisher and Koven, 2020).

675 The NCAR-NEON system also promotes reproducibility of research in alignment with the FAIR  
676 data principles (Wilkinson et al. 2016), addressing an ongoing challenge facing both ecology and  
677 geosciences (Powers and Hampton 2019; Culina et al. 2020; Kinkade and Shepherd 2021). The NCAR-  
678 NEON system makes it easy for researchers to share their research workflow as part of their publications,  
679 including accompanying code and data. The containerized system also reduces the time required to  
680 configure and run other researchers' workflows, thereby facilitating the process of reproducing previous  
681 studies and expanding existing workflows to answer new research questions.

682 In addition to enabling opportunities for research with NCAR models, the NCAR-NEON system  
683 also facilitates access to NEON data which can be used for observationally based research or research  
684 using other models. For example, the gap-filled micrometeorological data and partitioned flux data  
685 products provided in the NCAR-NEON system could be used in other projects related to ecological  
686 forecasting and model evaluation that focuses on ecological processes and land model simulations (Best  
687 et al. 2015; Collier et al. 2018; Eyring et al. 2019; Lewis et al. 2022). As latencies in publishing NEON  
688 data are reduced, we intend to provide updated input and evaluation data to the NCAR-NEON system to  
689 enable near-real time hindcasts of ecosystem states and fluxes. In short, we see the information that is  
690 being generated through this activity as a resource to meet data-requirements of the broader Earth  
691 system science community.

#### 692 ***4.3 Opportunities enabled for teaching***

693 The NCAR-NEON system makes it easy to run and visualize site-level simulations that can be  
694 integrated into classroom settings, and the NEON Observatory design provides a unique opportunity for  
695 students to access data from world class field research sites and instrumentation in a variety of  
696 ecosystems. Here we highlight two capacities in which this tool can be integrated into classroom  
697 activities, complementing other learning modules that integrate ecological data with modeling tools, such  
698 as those from Project EDDIE (e.g., Carey et al. 2020, O'Reilly et al 2017) to broaden exposure to large

699 datasets, ecological modeling, and systems thinking. The first is an interactive web-based visualization  
700 tool (Table 2). This tool does not require any software or data downloads, allowing students to access  
701 and explore NEON and CTSM data without running any simulations. Students can explore and compare  
702 observational and simulated data for numerous fluxes at different temporal scales from 45 terrestrial  
703 NEON sites (Table S1). Classroom modules can be developed to probe various ecological questions,  
704 including comparisons across sites, how fluxes change seasonally, and quantification of interannual  
705 variability. Instructors can also use this tool to highlight differences between models and observations,  
706 helping students to better understand how we measure, simulate, and predict ecosystem processes.

707 A second opportunity for classroom activities is to run simulations using the NCAR-NEON system  
708 within the CESM-Lab container. The flexible cyberinfrastructure, short simulation run times (typically less  
709 than 10 minutes), and simplified coding requirements facilitate running simulations for classroom  
710 applications. Technical challenges are minimal and can be reduced by using a computer lab with Docker  
711 pre-installed and computers that have sufficient memory and space requirements for data downloads, or  
712 by using larger-scale computing resources like university clusters or cloud computing resources. Once  
713 access to the containerized computing environment is established, students can use the available  
714 tutorials to run NEON tower simulations at the site of their choice and evaluate simulated fluxes against  
715 observations (Table 2).

716 The NCAR-NEON system is flexible, allowing instructors to easily make additional customizations  
717 for their classes. As an example, this cyberinfrastructure tool was used in a graduate level Land-Climate  
718 Interactions Course at Auburn University in the 2021-2022 academic year. First, students performed  
719 CTSM simulations for the Talladega National Forest site (TALL), the NEON site closest to Auburn  
720 University, and compared latent heat flux simulated by CTSM with the NEON measurements using  
721 system tutorials. Next, students were divided into two project groups focusing on either TALL or Ordway-  
722 Swisher Biological Station (OSBS) sites to conduct parameter perturbation experiments using a tutorial  
723 developed by the instructor. Students collected the relevant parameter values from the literature, updated  
724 model parameter files, and performed ten CTSM simulations at each site, finding that GPP was more  
725 sensitive to the selected parameters than latent heat fluxes. These classroom exercises were paired with  
726 a visit to the TALL site to enrich student's experiences and motivate them to design their own  
727 investigation and experiments. Exposure to the NCAR-NEON system has motivated graduate students to  
728 contribute analyses, tutorials, and additional resources to the broader community. For example, one  
729 graduate student compared NEON precipitation measurements with nearby NOAA sites, helping to  
730 identify potentially problematic NEON sensors (Section 4.1), while another is developing a model for  
731 estimating aboveground biomass using ground-based NEON data and remote sensing measurements  
732 (Narine et al. 2020). These examples highlight how the NCAR-NEON system is inspiring the next  
733 generation of scientists.

## 734 **Conclusion**

735 Deeper engagement of diverse scientific communities, removing technical barriers, and  
736 increasing access to research data and tools is critical to advance Earth system science, prediction, and  
737 understanding of ecosystem responses to global change. By developing cyberinfrastructure tools that  
738 facilitate the easy and rapid use of measurements, models, and computing tools, the NCAR-NEON  
739 system aims to enable this convergence of climate and ecological sciences and facilitates the  
740 development and testing of data-driven and model-enabled scientific hypotheses. The system provides a  
741 computationally simplified platform for scientific discovery and for rigorous evaluation and improvement of  
742 model simulations and observational data at NEON tower sites. By facilitating community engagement in  
743 modeling and observing terrestrial ecosystems, cyberinfrastructure tools like this are a key component for  
744 building a more intellectually diverse workforce for global change research and Earth system science.

## 745 **Code and Data availability**

746 Datasets created as part of this project are available as a NEON prototype dataset and archived at  
747 NCAR's Geoscience Data Exchange (GDEX) <https://doi.org/10.5065/tmmj-sj66>. CTSM code is available  
748 through the CTSM github page and archived at <https://doi.org/10.5281/zenodo.7342803>. Post processing  
749 scripts that used to make figures in this manuscript are available at:  
750 [https://github.com/NCAR/neon\\_scripts](https://github.com/NCAR/neon_scripts).

## 751 **Author Contributions**

752 All authors contributed to writing and review of the software and manuscript. GBB and MSC contributed to  
753 funding acquisition. DLL, WRW, NS, GBB, DD, DL, and MSC contributed to conceptualization and data  
754 curation. DLL, WRW, NS, and DD contributed to formal analysis, software development, validation, and  
755 visualization.

## 756 **Competing Interests**

757 The authors have no competing interests to declare.

## 758 **Acknowledgements**

759 Significant contributions to this work were made by Jim Edwards, Brian Dobbins, Erik Kluzek, Cove  
760 Sturtevant, and Giorgio Scorzelli. We also appreciate the support of the National Science Data Fabric  
761 (NSDF) platform. This material is based upon work supported by the National Center for Atmospheric  
762 Research, which is a major facility sponsored by the National Science Foundation (NSF) under  
763 Cooperative Agreement No. 1852977 with additional support from NSF award number 2039932. The

764 National Ecological Observatory Network is a program sponsored by the NSF and operated under  
765 cooperative agreement by Battelle. WRW was also supported by NSF award numbers 1926413,  
766 2031238, and 2120804. SK's contributions were supported by the USDA NIFA grant 2020-67021-32476.  
767 KMD's contributions were supported by NSF award numbers 1702379 and 2044818 and the USDA NIFA,  
768 Hatch project 1025001. VP's contributions were funded in part by NSF OAC award 2138811, NSF CI CoE  
769 Award 2127548, and the Intel oneAPI Center of Excellence at the University of Utah, using resources  
770 from the Chameleon, Cloudlab, CloudBank, Fabric, and ACCESS testbeds supported by the National  
771 Science Foundation.

772 **References**

- 773 Ayres, E., Colliander, A., Cosh, M. H., Roberti, J. A., Simkin, S., and Genazzio, M. A.: Validation of  
774 SMAP Soil Moisture at Terrestrial National Ecological Observatory Network (NEON) Sites Show  
775 Potential for Soil Moisture Retrieval in Forested Areas, *IEEE Journal of Selected Topics in*  
776 *Applied Earth Observations and Remote Sensing*, 14, 10903-10918,  
777 10.1109/jstars.2021.3121206, 2021.
- 778 Balch, J. K., Nagy, R. C., and Halpern, B. S.: NEON is seeding the next revolution in ecology,  
779 *Frontiers in Ecology and the Environment*, 18, 3-3, 10.1002/fee.2152, 2020.
- 780 Beringer, J., Moore, C. E., Cleverly, J., Campbell, D. I., Cleugh, H., De Kauwe, M. G., Kirschbaum,  
781 M. U. F., Griebel, A., Grover, S., Huete, A., Hutley, L. B., Laubach, J., van Niel, T., Arndt, S. K.,  
782 Bennett, A. C., Cernusak, L. A., Eamus, D., Ewenz, C. M., Goodrich, J. P., ... Woodgate, W. (2022).  
783 Bridge to the future: Important lessons from 20 years of ecosystem observations made by the  
784 OzFlux network. *Global Change Biology*, 28, 3489– 3514. <https://doi.org/10.1111/gcb.16141>
- 785 Best, M. J., Abramowitz, G., Johnson, H. R., Pitman, A. J., Balsamo, G., Boone, A., Cuntz, M.,  
786 Decharme, B., Dirmeyer, P. A., Dong, J., Ek, M., Guo, Z., Haverd, V., van den Hurk, B. J. J.,  
787 Nearing, G. S., Pak, B., Peters-Lidard, C., Santanello, J. A., Stevens, L., and Vuichard, N.: The  
788 Plumbing of Land Surface Models Benchmarking Model Performance, *J Hydrometeorol*, 16,  
789 1425-1442, 2015.
- 790 Birch, L., Schwalm, C. R., Natali, S., Lombardozzi, D., Keppel-Aleks, G., Watts, J., Lin, X., Zona, D.,  
791 Oechel, W., Sachs, T., Black, T. A., and Rogers, B. M.: Addressing biases in Arctic–boreal carbon  
792 cycling in the Community Land Model Version 5, *Geoscientific Model Development*, 14, 3361-  
793 3382, 10.5194/gmd-14-3361-2021, 2021.
- 794 Bonan, G.: *Ecological climatology: concepts and applications*, 3, Cambridge University Press,  
795 Cambridge, 2015.
- 796 Bonan, G.: *Climate change and terrestrial ecosystem modeling*, Cambridge University Press,  
797 Cambridge, 2019.
- 798 Bonan, G. B.: *A Land Surface Model (LSM Version 1.0) for Ecological, Hydrological, and*  
799 *Atmospheric Studies: Technical Description and User's Guide (No. NCAR/TN-417+STR)*,  
800 University Corporation for Atmospheric Research, 10.5065/D6DF6P5X, 1996.
- 801 Bonan, G. B. and Doney, S. C.: Climate, ecosystems, and planetary futures: The challenge to  
802 predict life in Earth system models, *Science*, 359, 10.1126/science.aam8328, 2018.
- 803 Bonan, G. B., Davis, K. J., Baldocchi, D., Fitzjarrald, D., and Neumann, H.: Comparison of the  
804 NCAR LSM1 land surface model with BOREAS aspen and jack pine tower fluxes, *Journal of*  
805 *Geophysical Research-Atmospheres*, 102, 29065-29075, 10.1029/96jd03095, 1997.

806 Bonan, G. B., Oleson, K. W., Fisher, R. A., Lasslop, G., and Reichstein, M.: Reconciling leaf  
807 physiological traits and canopy flux data: Use of the TRY and FLUXNET databases in the  
808 Community Land Model version 4, *Journal of Geophysical Research: Biogeosciences*, 117,  
809 G02026, 10.1029/2011jg001913, 2012.

810 Bonan, G. B., Lawrence, P. J., Oleson, K. W., Levis, S., Jung, M., Reichstein, M., Lawrence, D. M.,  
811 and Swenson, S. C.: Improving canopy processes in the Community Land Model version 4  
812 (CLM4) using global flux fields empirically inferred from FLUXNET data, *J. Geophys. Res.*, 116,  
813 G02014, 10.1029/2010jg001593, 2011.

814 Brock, F. V.: A Nonlinear Filter to Remove Impulse Noise from Meteorological Data, *Journal of*  
815 *Atmospheric and Oceanic Technology*, 3, 51-58, 10.1175/1520-  
816 0426(1986)003<0051:Anftri>2.0.Co;2, 1986.

817 Burns, S. P., Swenson, S. C., Wieder, W. R., Lawrence, D. M., Bonan, G. B., Knowles, J. F., and  
818 Blanken, P. D.: A Comparison of the Diel Cycle of Modeled and Measured Latent Heat Flux  
819 During the Warm Season in a Colorado Subalpine Forest, *Journal of Advances in Modeling Earth*  
820 *Systems*, 10, 617-651, 10.1002/2017ms001248, 2018.

821 Carey, CC, Farrell, KJ, Hounshell, AG, O'Connell, K. Macrosystems EDDIE teaching modules  
822 significantly increase ecology students' proficiency and confidence working with ecosystem  
823 models and use of systems thinking. *Ecol Evol.* 2020; 10: 12515– 12527.  
824 <https://doi.org/10.1002/ece3.6757>

825 Carey, C.C., Darner Gougis, R., Klug, J. L., O'Reilly, C. M., and Richardson, D. C. 2015. [A model](#)  
826 [for using environmental data-driven inquiry and exploration to teach limnology to](#)  
827 [undergraduates](#). *Limnology and Oceanography Bulletin* 24(2): 2-5. doi:10.1002/lob.10020

828 Collier, N., Hoffman, F. M., Lawrence, D. M., Keppel-Aleks, G., Koven, C. D., Riley, W. J., Mu, M.  
829 Q., and Randerson, J. T.: The International Land Model Benchmarking (ILAMB) System: Design,  
830 Theory, and Implementation, *Journal of Advances in Modeling Earth Systems*, 10, 2731-2754,  
831 10.1029/2018ms001354, 2018.

832 Culina, A., van den Berg, I., Evans, S., and Sanchez-Tojar, A.: Low availability of code in ecology:  
833 A call for urgent action, *PLoS Biol*, 18, e3000763, 10.1371/journal.pbio.3000763, 2020.

834 Danabasoglu, G., Lamarque, J.-F., Bacmeister, J., Bailey, D. A., DuVivier, A. K., Edwards, J.,  
835 Emmons, L. K., Fasullo, J., Garcia, R., Gettelman, A., Hannay, C., Holland, M. M., Large, W. G.,  
836 Lauritzen, P. H., Lawrence, D. M., Lenaerts, J. T. M., Lindsay, K., Lipscomb, W. H., Mills, M. J.,  
837 Neale, R., Oleson, K. W., Otto-Bliesner, B., Phillips, A. S., Sacks, W., Tilmes, S., van Kampenhout,  
838 L., Vertenstein, M., Bertini, A., Dennis, J., Deser, C., Fischer, C., Fox-Kemper, B., Kay, J. E.,  
839 Kinnison, D., Kushner, P. J., Larson, V. E., Long, M. C., Mickelson, S., Moore, J. K., Nienhouse, E.,  
840 Polvani, L., Rasch, P. J., and Strand, W. G.: The Community Earth System Model Version 2  
841 (CESM2), *Journal of Advances in Modeling Earth Systems*, 12, e2019MS001916,  
842 10.1029/2019ms001916, 2020.

843 Deardorff, J. W.: Efficient prediction of ground surface temperature and moisture, with  
844 inclusion of a layer of vegetation, *Journal of Geophysical Research*, 83, 1889-1903,  
845 10.1029/JC083iC04p01889, 1978.

846 Dickinson, R. E., Henderson-Sellers, A., and Kennedy, P. J.: Biosphere-atmosphere Transfer  
847 Scheme (BATS) Version 1e as Coupled to the NCAR Community Climate Model (No. NCAR/TN-  
848 387+STR). , University Corporation for Atmospheric Research, 10.5065/D67W6959, 1993.

849 Dickinson, R. E., Henderson-Sellers, A., Kennedy, P. J., &, and Wilson, M. F.: Biosphere-  
850 atmosphere Transfer Scheme (BATS) for the NCAR Community Climate Model (No. NCAR/TN-  
851 275-+STR). , 72, 10.5065/D6668B58, 1986.

852 Durden, D. J., Metzger, S., Chu, H., Collier, N., Davis, K. J., Desai, A. R., Kumar, J., Wieder, W. R.,  
853 Xu, M., and Hoffman, F. M., Nichols, J., Verastegui, B., Maccabe, A. B., Hernandez, O., Parete-  
854 Koon, S., and Ahearn, T. (Eds.): *Automated Integration of Continental-Scale Observations in  
855 Near-Real Time for Simulation and Analysis of Biosphere–Atmosphere Interactions*, Springer  
856 International Publishing, Cham, 204-225 pp., 10.1007/978-3-030-63393-6\_14, 2020.

857 Eyring, V., Cox, P. M., Flato, G. M., Gleckler, P. J., Abramowitz, G., Caldwell, P., Collins, W. D.,  
858 Gier, B. K., Hall, A. D., Hoffman, F. M., Hurtt, G. C., Jahn, A., Jones, C. D., Klein, S. A., Krasting, J.  
859 P., Kwiatkowski, L., Lorenz, R., Maloney, E., Meehl, G. A., Pendergrass, A. G., Pincus, R., Ruane,  
860 A. C., Russell, J. L., Sanderson, B. M., Santer, B. D., Sherwood, S. C., Simpson, I. R., Stouffer, R. J.,  
861 and Williamson, M. S.: Taking climate model evaluation to the next level, *Nature Climate  
862 Change*, 9, 102-110, 10.1038/s41558-018-0355-y, 2019.

863 Falge, E., Baldocchi, D., Olson, R., Anthoni, P., Aubinet, M., Bernhofer, C., Burba, G., Ceulemans,  
864 R., Clement, R., Dolman, H., Granier, A., Gross, P., Grünwald, T., Hollinger, D., Jensen, N.-O.,  
865 Katul, G., Keronen, P., Kowalski, A., Ta Lai, C., Law, B. E., Meyers, T., Moncrieff, J., Moors, E.,  
866 William Munger, J., Pilegaard, K., Rannik, Ü., Rebmann, C., Suyker, A., Tenhunen, J., Tu, K.,  
867 Verma, S., Vesala, T., Wilson, K., and Wofsy, S.: Gap filling strategies for long term energy flux  
868 data sets, *Agricultural and Forest Meteorology*, 107, 71-77, 10.1016/s0168-1923(00)00235-5,  
869 2001.

870 Fer, I., Gardella, A. K., Shiklomanov, A. N., Campbell, E. E., Cowdery, E. M., De Kauwe, M. G.,  
871 Desai, A., Duveneck, M. J., Fisher, J. B., Haynes, K. D., Hoffman, F. M., Johnston, M. R., Kooper,  
872 R., LeBauer, D. S., Mantooth, J., Parton, W. J., Poulter, B., Quaife, T., Raiho, A., Schaefer, K.,  
873 Serbin, S. P., Simkins, J., Wilcox, K. R., Viskari, T., and Dietze, M. C.: Beyond ecosystem  
874 modeling: A roadmap to community cyberinfrastructure for ecological data-model integration,  
875 *Glob Chang Biol*, 27, 13-26, 10.1111/gcb.15409, 2021.

876 Finkenbiner, C. E., Li, B., Spencer, L., Butler, Z., Haagsma, M., Fiorella, R. P., Allen, S. T.,  
877 Anderegg, W., Still, C. J., Noone, D., Bowen, G. J., and Good, S. P.: The NEON Daily Isotopic  
878 Composition of Environmental Exchanges Dataset, *Scientific Data*, 9, 353, 10.1038/s41597-022-  
879 01412-4, 2022.



880 Fisher, R. A. and Koven, C. D.: Perspectives on the Future of Land Surface Models and the  
881 Challenges of Representing Complex Terrestrial Systems, *Journal of Advances in Modeling Earth*  
882 *Systems*, 12, e2018MS001453, 10.1029/2018ms001453, 2020.

883 Hinckley, E.-L. S., Anderson, S. P., Baron, J. S., Blanken, P. D., Bonan, G. B., Bowman, W. D.,  
884 Elmendorf, S. C., Fierer, N., Fox, A. M., Goodman, K. J., Jones, K. D., Lombardozzi, D. L., Lunch, C.  
885 K., Neff, J. C., SanClements, M. D., Suding, K. N., and Wieder, W. R.: Optimizing Available  
886 Network Resources to Address Questions in Environmental Biogeochemistry, *BioScience*, 66,  
887 317-326, 10.1093/biosci/biw005, 2016.

888 Hurrell, J. W., Holland, M. M., Gent, P. R., Ghan, S., Kay, J. E., Kushner, P. J., Lamarque, J. F.,  
889 Large, W. G., Lawrence, D., Lindsay, K., Lipscomb, W. H., Long, M. C., Mahowald, N., Marsh, D.  
890 R., Neale, R. B., Rasch, P., Vavrus, S., Vertenstein, M., Bader, D., Collins, W. D., Hack, J. J., Kiehl,  
891 J., and Marshall, S.: The Community Earth System Model: A Framework for Collaborative  
892 Research, *Bulletin of the American Meteorological Society*, 94, 1339-1360, 10.1175/bams-d-12-  
893 00121.1, 2013.

894 Jung, M., Schwalm, C., Migliavacca, M., Walther, S., Camps-Valls, G., Koirala, S., Anthoni, P.,  
895 Besnard, S., Bodesheim, P., Carvalhais, N., Chevallier, F., Gans, F., Goll, D. S., Haverd, V., Köhler,  
896 P., Ichii, K., Jain, A. K., Liu, J., Lombardozzi, D., Nabel, J. E. M. S., Nelson, J. A., O'Sullivan, M.,  
897 Pallandt, M., Papale, D., Peters, W., Pongratz, J., Rödenbeck, C., Sitch, S., Tramontana, G.,  
898 Walker, A., Weber, U., and Reichstein, M.: Scaling carbon fluxes from eddy covariance sites to  
899 globe: synthesis and evaluation of the FLUXCOM approach, *Biogeosciences*, 17, 1343-1365,  
900 10.5194/bg-17-1343-2020, 2020.

901 Keetz, L. T., Lieungh, E., Karimi-Asli, K., Geange, S. R., Gelati, E., Tang, H., et al. (2023). Climate-  
902 ecosystem modelling made easy: The Land Sites Platform. *Global Change Biology*, 29, 4440-  
903 4452. <https://doi.org/10.1111/gcb.16808>

904 Kinkade, D. and Shepherd, A.: Geoscience data publication: Practices and perspectives on  
905 enabling the FAIR guiding principles, *Geoscience Data Journal*, 9, 177-186, 10.1002/gdj3.120,  
906 2021.

907 Koven, C. D., Knox, R. G., Fisher, R. A., Chambers, J. Q., Christoffersen, B. O., Davies, S. J., Detto,  
908 M., Dietze, M. C., Faybishenko, B., Holm, J., Huang, M., Kovenock, M., Kueppers, L. M., Lemieux,  
909 G., Massoud, E., McDowell, N. G., Muller-Landau, H. C., Needham, J. F., Norby, R. J., Powell, T.,  
910 Rogers, A., Serbin, S. P., Shuman, J. K., Swann, A. L. S., Varadharajan, C., Walker, A. P., Wright, S.  
911 J., and Xu, C.: Benchmarking and parameter sensitivity of physiological and vegetation dynamics  
912 using the Functionally Assembled Terrestrial Ecosystem Simulator (FATES) at Barro Colorado  
913 Island, Panama, *Biogeosciences*, 17, 3017-3044, 10.5194/bg-17-3017-2020, 2020.

914 Kyker-Snowman, E., Lombardozzi, D. L., Bonan, G. B., Cheng, S. J., Dukes, J. S., Frey, S. D.,  
915 Jacobs, E. M., McNellis, R., Rady, J. M., Smith, N. G., Thomas, R. Q., Wieder, W. R., and Grandy,  
916 A. S.: Increasing the spatial and temporal impact of ecological research: A roadmap for

917 integrating a novel terrestrial process into an Earth system model, *Glob Chang Biol*, 28, 665-  
918 684, 10.1111/gcb.15894, 2021.

919 Lawrence, D. M., Fisher, R. A., Koven, C. D., Oleson, K. W., Swenson, S. C., Bonan, G., Collier, N.,  
920 Ghimire, B., Kampenhout, L., Kennedy, D., Kluzek, E., Lawrence, P. J., Li, F., Li, H., Lombardozzi,  
921 D., Riley, W. J., Sacks, W. J., Shi, M., Vertenstein, M., Wieder, W. R., Xu, C., Ali, A. A., Badger, A.  
922 M., Bisht, G., Broeke, M., Brunke, M. A., Burns, S. P., Buzan, J., Clark, M., Craig, A., Dahlin, K.,  
923 Drewniak, B., Fisher, J. B., Flanner, M., Fox, A. M., Gentine, P., Hoffman, F., Keppel-Aleks, G.,  
924 Knox, R., Kumar, S., Lenaerts, J., Leung, L. R., Lipscomb, W. H., Lu, Y., Pandey, A., Pelletier, J. D.,  
925 Perket, J., Randerson, J. T., Ricciuto, D. M., Sanderson, B. M., Slater, A., Subin, Z. M., Tang, J.,  
926 Thomas, R. Q., Val Martin, M., and Zeng, X.: The Community Land Model Version 5: Description  
927 of New Features, Benchmarking, and Impact of Forcing Uncertainty, *Journal of Advances in*  
928 *Modeling Earth Systems*, 11, 4245-4287, 10.1029/2018ms001583, 2019.

929 LeBauer, D. S., Wang, D., Richter, K. T., Davidson, C. C., and Dietze, M. C.: Facilitating feedbacks  
930 between field measurements and ecosystem models, *Ecological Monographs*, 83, 133-154,  
931 10.1890/12-0137.1, 2013.

932 Levis, S., Bonan, G. B., Vertenstein, M., and Oleson, K. W.: The Community Land Model's  
933 Dynamic Global Vegetation Model (CLM-DGVM): Technical description and user's guide. NCAR  
934 Technical Note NCAR/TN-459+IA., National Center for Atmospheric Research, Boulder, CO. ,  
935 10.5065/D6P26W36, 2004.

936 Lewis, A. S. L., Rollinson, C. R., Allyn, A. J., Ashander, J., Brodie, S., Brookson, C. B., Collins, E.,  
937 Dietze, M. C., Gallinat, A. S., Juvigny-Khenafou, N., Koren, G., McGlenn, D. J., Moustahfid, H.,  
938 Peters, J. A., Record, N. R., Robbins, C. J., Tonkin, J., and Wardle, G. M.: The power of forecasts  
939 to advance ecological theory, *Methods in Ecology and Evolution*, n/a, 10.1111/2041-  
940 210x.13955, 2022.

941 Li, X., Melaas, E., Carrillo, C. M., Ault, T., Richardson, A. D., Lawrence, P., Friedl, M. A.,  
942 Seyednasrollah, B., Lawrence, D. M., and Young, A. M.: A Comparison of Land Surface  
943 Phenology in the Northern Hemisphere Derived from Satellite Remote Sensing and the  
944 Community Land Model, *J Hydrometeorol*, 23, 859-873, 10.1175/jhm-d-21-0169.1, 2022.

945 Lombardozzi, D. L., Bonan, G. B., Smith, N. G., Dukes, J. S., and Fisher, R. A.: Temperature  
946 acclimation of photosynthesis and respiration: A key uncertainty in the carbon cycle-climate  
947 feedback, *Geophysical Research Letters*, 42, 8624-8631, 10.1002/2015GL065934., 2015.

948 Metzger, S., Ayres, E., Durden, D., Florian, C., Lee, R., Lunch, C., Luo, H., Pingingtha-Durden, N.,  
949 Roberti, J. A., SanClements, M., Sturtevant, C., Xu, K., and Zulueta, R. C.: From NEON Field Sites  
950 to Data Portal: A Community Resource for Surface–Atmosphere Research Comes Online,  
951 *Bulletin of the American Meteorological Society*, 100, 2305-2325, 10.1175/bams-d-17-0307.1,  
952 2019.

953 Miles, A., jakirkham, Bussonnier, M., Moore, J., Orfanos, D. P., Fulton, A., Bourbeau, J., Lee, G.,  
954 Patel, Z., Bennett, D., Rocklin, M., Abernathey, R., Andrade, E. S. d., Durant, M., Schut, V.,  
955 Dussin, R., Kristensen, M. R. B., Chaudhary, S., Barnes, C., Nunez-Iglesias, J., Williams, B., Mohar,  
956 B., Noyes, C., Bell, R., hailiangzhang, shikharsg, Jelenak, A., Sansal, A., and Banahirwe, A.: zarr-  
957 developers/zarr-python: v2.13.0 Zenodo, 10.5281/zenodo.7104413, 2022.

958 Moffat, A. M., Papale, D., Reichstein, M., Hollinger, D. Y., Richardson, A. D., Barr, A. G.,  
959 Beckstein, C., Braswell, B. H., Churkina, G., Desai, A. R., Falge, E., Gove, J. H., Heimann, M., Hui,  
960 D., Jarvis, A. J., Kattge, J., Noormets, A., and Stauch, V. J.: Comprehensive comparison of gap-  
961 filling techniques for eddy covariance net carbon fluxes, *Agricultural and Forest Meteorology*,  
962 147, 209-232, 10.1016/j.agrformet.2007.08.011, 2007.

963 Moon, M., Richardson, A. D., Milliman, T., and Friedl, M. A.: A high spatial resolution land  
964 surface phenology dataset for AmeriFlux and NEON sites, *Scientific Data*, 9, 448,  
965 10.1038/s41597-022-01570-5, 2022.

966 Narine, L. L., Popescu, S. C., and Malambo, L.: Using ICESat-2 to Estimate and Map Forest  
967 Aboveground Biomass: A First Example, 10.3390/rs12111824, 2020.

968 National Academies of Sciences, E. and Medicine: Next Generation Earth Systems Science at the  
969 National Science Foundation, The National Academies Press, Washington, DC, 136 pp.,  
970 10.17226/26042, 2022.

971 NEON (National Ecological Observatory Network). NCAR-NEON gap-filled data, v2  
972 (10.48443/8w20-r938). <https://doi.org/10.48443/8w20-r938>. Dataset accessed from  
973 <https://data.neonscience.org> on February 13, 2023

974 Novick, K. A., Biederman, J. A., Desai, A. R., Litvak, M. E., Moore, D. J. P., Scott, R. L., & Torn, M.  
975 S. (2018). The AmeriFlux network: A coalition of the willing. *Agricultural And Forest*  
976 *Meteorology*, 249, 444-456. doi: <https://doi.org/10.1016/j.agrformet.2017.10.009>

977 Oleson, K., Lawrence, D., Bonan, G., Drewniak, B., Huang, M., Koven, C., Levis, S., Li, F., Riley,  
978 W., and Subin, Z.: Technical description of version 4.0 of the Community Land Model (CLM),  
979 NCAR Tech, Notes (NCAR/TN-478+ STR), 605, 2010.

980 Oleson, K., Dai, Y., Bonan, G. B., Bosilovich, M., Dickinson, R. E., Dirmeyer, P., Hoffman, F.,  
981 Houser, P., Levis, S., Niu, G.-Y., Thornton, P., Vertenstein, M., Z.-L., Y., and Zeng, X.: Technical  
982 Description of the Community Land Model (CLM) (No. NCAR/TN-461+STR), University  
983 Corporation for Atmospheric Research, 185, 10.5065/D6N877R0, 2004.

984 Oleson, K., Lawrence, D. M., Bonan, G. B., Drewniak, B., Huang, M., Koven, C. D., Levis, S., Li, F.,  
985 Riley, W. J., Subin, Z. M., Swenson, S., Thornton, P. E., Bozbiyik, A., Fisher, R., Heald, C. L.,  
986 Kluzek, E., Lamarque, J. F., Lawrence, P. J., Leung, L. R., Lipscomb, W., Muszala, S. P., Ricciuto, D.  
987 M., Sacks, W. J., Sun, Y., Tang, J., and Yang, Z. L.: Technical description of version 4.5 of the

988 Community Land Model (CLM). NCAR Technical Note NCAR/TN-503+STR, 10.5065/D6RR1W7M,  
989 2013.

990 O'Reilly, C.M., Gougis, R.D., Klug, J.L., Carey, C.C., Richardson, D.C., Bader, N.E., Soule, D.C.,  
991 Castendyk, D., Meixner T., Stromberg, J., Weathers, K.C., and W. Hunter. 2017. Using large data  
992 sets for open-ended inquiry in undergraduate science classrooms. *Bioscience* 67:12:1052-1061.  
993 doi.org/10.1093/biosci/bix118

994 Pastorello, G., Trotta, C., Canfora, E., Chu, H., Christianson, D., Cheah, Y.-W., Poindexter, C.,  
995 Chen, J., Elbashandy, A., Humphrey, M., Isaac, P., Polidori, D., Reichstein, M., Ribeca, A., van  
996 Ingen, C., Vuichard, N., Zhang, L., Amiro, B., Ammann, C., Arain, M. A., Ardö, J., Arkebauer, T.,  
997 Arndt, S. K., Arriga, N., Aubinet, M., Aurela, M., Baldocchi, D., Barr, A., Beamesderfer, E.,  
998 Marchesini, L. B., Bergeron, O., Beringer, J., Bernhofer, C., Berveiller, D., Billesbach, D., Black, T.  
999 A., Blanken, P. D., Bohrer, G., Boike, J., Bolstad, P. V., Bonal, D., Bonnefond, J.-M., Bowling, D. R.,  
1000 Bracho, R., Brodeur, J., Brümmer, C., Buchmann, N., Burban, B., Burns, S. P., Buysse, P., Cale, P.,  
1001 Cavagna, M., Cellier, P., Chen, S., Chini, I., Christensen, T. R., Cleverly, J., Collalti, A., Consalvo,  
1002 C., Cook, B. D., Cook, D., Coursolle, C., Cremonese, E., Curtis, P. S., D'Andrea, E., da Rocha, H.,  
1003 Dai, X., Davis, K. J., Cinti, B. D., Grandcourt, A. d., Ligne, A. D., De Oliveira, R. C., Delpierre, N.,  
1004 Desai, A. R., Di Bella, C. M., Tommasi, P. d., Dolman, H., Domingo, F., Dong, G., Dore, S., Duce,  
1005 P., Dufrêne, E., Dunn, A., Dušek, J., Eamus, D., Eichelmann, U., ElKhidir, H. A. M., Eugster, W.,  
1006 Ewenz, C. M., Ewers, B., Famulari, D., Fares, S., Feigenwinter, I., Feitz, A., Fensholt, R., Filippa,  
1007 G., Fischer, M., Frank, J., Galvagno, M., Gharun, M., Gianelle, D., Gielen, B., Gioli, B., Gitelson,  
1008 A., Goded, I., Goeckede, M., Goldstein, A. H., Gough, C. M., Goulden, M. L., Graf, A., Griebel, A.,  
1009 Gruening, C., Grünwald, T., Hammerle, A., Han, S., Han, X., Hansen, B. U., Hanson, C., Hatakka,  
1010 J., He, Y., Hehn, M., Heinesch, B., Hinko-Najera, N., Hörtnagl, L., Hutley, L., Ibrom, A., Ikawa, H.,  
1011 Jackowicz-Korczynski, M., Janouš, D., Jans, W., Jassal, R., Jiang, S., Kato, T., Khomik, M., Klatt, J.,  
1012 Knohl, A., Knox, S., Kobayashi, H., Koerber, G., Kolle, O., Kosugi, Y., Kotani, A., Kowalski, A.,  
1013 Kruijt, B., Kurbatova, J., Kutsch, W. L., Kwon, H., Launiainen, S., Laurila, T., Law, B., Leuning, R.,  
1014 Li, Y., Liddell, M., Limousin, J.-M., Lion, M., Liska, A. J., Lohila, A., López-Ballesteros, A., López-  
1015 Blanco, E., Loubet, B., Loustau, D., Lucas-Moffat, A., Lüers, J., Ma, S., Macfarlane, C., Magliulo,  
1016 V., Maier, R., Mammarella, I., Manca, G., Marcolla, B., Margolis, H. A., Marras, S., Massman, W.,  
1017 Mastepanov, M., Matamala, R., Matthes, J. H., Mazzenga, F., McCaughey, H., McHugh, I.,  
1018 McMillan, A. M. S., Merbold, L., Meyer, W., Meyers, T., Miller, S. D., Minerbi, S., Moderow, U.,  
1019 Monson, R. K., Montagnani, L., Moore, C. E., Moors, E., Moreaux, V., Moureaux, C., Munger, J.  
1020 W., Nakai, T., Neiryneck, J., Nesic, Z., Nicolini, G., Noormets, A., Northwood, M., Nosetto, M.,  
1021 Nouvellon, Y., Novick, K., Oechel, W., Olesen, J. E., Ourcival, J.-M., Papuga, S. A., Parmentier, F.-  
1022 J., Paul-Limoges, E., Pavelka, M., Peichl, M., Pendall, E., Phillips, R. P., Pilegaard, K., Pirk, N.,  
1023 Posse, G., Powell, T., Prasse, H., Prober, S. M., Rambal, S., Rannik, Ü., Raz-Yaseef, N., Rebmann,  
1024 C., Reed, D., Dios, V. R. d., Restrepo-Coupe, N., Reverter, B. R., Roland, M., Sabbatini, S., Sachs,  
1025 T., Saleska, S. R., Sánchez-Cañete, E. P., Sanchez-Mejia, Z. M., Schmid, H. P., Schmidt, M.,  
1026 Schneider, K., Schrader, F., Schroder, I., Scott, R. L., Sedlák, P., Serrano-Ortíz, P., Shao, C., Shi, P.,  
1027 Shironya, I., Siebicke, L., Šigut, L., Silberstein, R., Sirca, C., Spano, D., Steinbrecher, R., Stevens,  
1028 R. M., Sturtevant, C., Suyker, A., Tagesson, T., Takanashi, S., Tang, Y., Tapper, N., Thom, J.,  
1029 Tomassucci, M., Tuovinen, J.-P., Urbanski, S., Valentini, R., van der Molen, M., van Gorsel, E.,

1030 van Huissteden, K., Varlagin, A., Verfaillie, J., Vesala, T., Vincke, C., Vitale, D., Vygodskaya, N.,  
1031 Walker, J. P., Walter-Shea, E., Wang, H., Weber, R., Westermann, S., Wille, C., Wofsy, S.,  
1032 Wohlfahrt, G., Wolf, S., Woodgate, W., Li, Y., Zampedri, R., Zhang, J., Zhou, G., Zona, D.,  
1033 Agarwal, D., Biraud, S., Torn, M., and Papale, D.: The FLUXNET2015 dataset and the ONEFlux  
1034 processing pipeline for eddy covariance data, *Scientific Data*, 7, 225, 10.1038/s41597-020-0534-  
1035 3, 2020.

1036 Powers, S. M. and Hampton, S. E.: Open science, reproducibility, and transparency in ecology,  
1037 *Ecol Appl*, 29, e01822, 10.1002/eap.1822, 2019.

1038 Reichstein, M., Falge, E., Baldocchi, D., Papale, D., Aubinet, M., Berbigier, P., Bernhofer, C.,  
1039 Buchmann, N., Gilmanov, T., Granier, A., Grunwald, T., Havrankova, K., Ilvesniemi, H., Janous,  
1040 D., Knohl, A., Laurila, T., Lohila, A., Loustau, D., Matteucci, G., Meyers, T., Miglietta, F., Ourcival,  
1041 J.-M., Pumpanen, J., Rambal, S., Rotenberg, E., Sanz, M., Tenhunen, J., Seufert, G., Vaccari, F.,  
1042 Vesala, T., Yakir, D., and Valentini, R.: On the separation of net ecosystem exchange into  
1043 assimilation and ecosystem respiration: review and improved algorithm, *Global Change Biology*,  
1044 11, 1424-1439, 10.1111/j.1365-2486.2005.001002.x, 2005.

1045 Richardson, A.D., Hufkens, K., Milliman, T., Aubrecht, D.M., Chen, M., Gray, J.M., Johnston,  
1046 M.R., Keenan, T.F., Klosterman, S.T., Kosmala, M., Melaas, E.K., Friedl, M.A., and Frohling, S.:  
1047 Tracking vegetation phenology across diverse North American biomes using PhenoCam  
1048 imagery, *Scientific Data* 5, Article number: 180028. doi:10.1038/sdata.2018.28, 2018.  
1049

1050 Richardson, L. F.: *Weather prediction by numerical process*, Cambridge University Press,  
1051 Cambridge 1922.

1052 Shepherd, A., Jones, M. B., Richard, S., Jarboe, N., Vieglais, D., Fils, D., Duerr, R., Verhey, C.,  
1053 Minch, M., Mecum, B., and Bentley, N.: *Science-on-Schema.org v1.3.0*, Zenodo,  
1054 10.5281/zenodo.6502539, 2022.

1055 Starkenburg, D., Metzger, S., Fochesatto, G. J., Alfieri, J. G., Gens, R., Prakash, A., and Cristóbal,  
1056 J.: Assessment of Despiking Methods for Turbulence Data in Micrometeorology, *Journal of*  
1057 *Atmospheric and Oceanic Technology*, 33, 2001-2013, 10.1175/jtech-d-15-0154.1, 2016.

1058 Stöckli, R., Lawrence, D. M., Niu, G. Y., Oleson, K. W., Thornton, P. E., Yang, Z. L., Bonan, G. B.,  
1059 Denning, A. S., and Running, S. W.: Use of FLUXNET in the Community Land Model  
1060 development, *Journal of Geophysical Research: Biogeosciences*, 113, 10.1029/2007jg000562,  
1061 2008.

1062 Swann, A. L. S., Laguë, M. M., Garcia, E. S., Field, J. P., Breshears, D. D., Moore, D. J. P., Saleska,  
1063 S. R., Stark, S. C., Villegas, J. C., Law, D. J., and Minor, D. M.: Continental-scale consequences of  
1064 tree die-offs in North America: identifying where forest loss matters most, *Environ Res Lett*, 13,  
1065 055014, 10.1088/1748-9326/aaba0f, 2018.

1066 Swenson, S. C., Clark, M., Fan, Y., Lawrence, D. M., and Perket, J.: Representing Intra-Hillslope  
1067 Lateral Subsurface Flow in the Community Land Model, *Journal of Advances in Modeling Earth*  
1068 *Systems*, 11, 10.1029/2019ms001833, 2019.

1069 van der Horst, S. V. J., Pitman, A. J., De Kauwe, M. G., Ukkola, A., Abramowitz, G., and Isaac, P.:  
1070 How representative are FLUXNET measurements of surface fluxes during temperature  
1071 extremes?, *Biogeosciences*, 16, 1829-1844, 10.5194/bg-16-1829-2019, 2019.

1072 Wieder, W. R., Knowles, J. F., Blanken, P. D., Swenson, S. C., and Suding, K. N.: Ecosystem  
1073 function in complex mountain terrain: Combining models and long-term observations to  
1074 advance process-based understanding, *Journal of Geophysical Research: Biogeosciences*, 122,  
1075 825-845, 10.1002/2016jg003704, 2017.

1076 Wilkinson, M. D., Dumontier, M., Aalbersberg, I. J., Appleton, G., Axton, M., Baak, A., Blomberg,  
1077 N., Boiten, J.-W., da Silva Santos, L. B., Bourne, P. E., Bouwman, J., Brookes, A. J., Clark, T.,  
1078 Crosas, M., Dillo, I., Dumon, O., Edmunds, S., Evelo, C. T., Finkers, R., Gonzalez-Beltran, A., Gray,  
1079 A. J. G., Groth, P., Goble, C., Grethe, J. S., Heringa, J., 't Hoen, P. A. C., Hooft, R., Kuhn, T., Kok,  
1080 R., Kok, J., Lusher, S. J., Martone, M. E., Mons, A., Packer, A. L., Persson, B., Rocca-Serra, P.,  
1081 Roos, M., van Schaik, R., Sansone, S.-A., Schultes, E., Sengstag, T., Slater, T., Strawn, G., Swertz,  
1082 M. A., Thompson, M., van der Lei, J., van Mulligen, E., Velterop, J., Waagmeester, A.,  
1083 Wittenburg, P., Wolstencroft, K., Zhao, J., and Mons, B.: The FAIR Guiding Principles for  
1084 scientific data management and stewardship, *Scientific Data*, 3, 160018,  
1085 10.1038/sdata.2016.18, 2016.

1086 Wozniak, M. C., Bonan, G. B., Keppel-Aleks, G., and Steiner, A. L.: Influence of Vertical  
1087 Heterogeneities in the Canopy Microenvironment on Interannual Variability of Carbon Uptake  
1088 in Temperate Deciduous Forests, *Journal of Geophysical Research: Biogeosciences*, 125,  
1089 e2020JG005658, 10.1029/2020jg005658, 2020.

1090 Wutzler, T., Lucas-Moffat, A., Migliavacca, M., Knauer, J., Sickel, K., Šigut, L., Menzer, O., and  
1091 Reichstein, M.: Basic and extensible post-processing of eddy covariance flux data with  
1092 REddyProc, *Biogeosciences*, 15, 5015-5030, 10.5194/bg-15-5015-2018, 2018.

1093